Nucleic Acids Research, 2017 **1**
doi: 10.1093/nar/gkx723

Abasic and oxidized ribonucleotides embedded in DNA are processed by human APE1 and not by RNase H2

Matilde Clarissa Malfatti[1,†], Sathya Balachander[2,†], Giulia Antoniali[1], Kyung Duk Koh[2,3], Christine Saint-Pierre[4], Didier Gasparutto[4], Hyongi Chon[5], Robert J. Crouch[5], Francesca Storici[2,*] and Gianluca Tell[1,*]

[1]Laboratory of Molecular Biology and DNA repair, Department of Medicine, University of Udine, Udine, Italy, [2]School of Biological Sciences, Georgia Institute of Technology, Atlanta, GA, USA, [3]Currently at the University of California, San Francisco, UCSF, School of Medicine, San Francisco, CA, USA, [4]Chimie Reconnaissance & Etude Assemblages Biologiques, Université Grenoble Alpes, SPrAM UMR5819 CEA CNRS UGA, INAC/CEA, Grenoble, France and [5]Developmental Biology Division, Eunice Kennedy Shriver National Institute of Child Health and Human Development, National Institutes of Health, Bethesda, MD, USA

Received November 01, 2016; Revised July 31, 2017; Editorial Decision August 06, 2017; Accepted August 11, 2017

ABSTRACT

Ribonucleoside 5′-monophosphates (rNMPs) are the most common non-standard nucleotides found in DNA of eukaryotic cells, with over 100 million rNMPs transiently incorporated in the mammalian genome per cell cycle. Human ribonuclease (RNase) H2 is the principal enzyme able to cleave rNMPs in DNA. Whether RNase H2 may process abasic or oxidized rNMPs incorporated in DNA is unknown. The base excision repair (BER) pathway is mainly responsible for repairing oxidized and abasic sites into DNA. Here we show that human RNase H2 is unable to process an abasic rNMP (rAP site) or a ribose 8oxoG (r8oxoG) site embedded in DNA. On the contrary, we found that recombinant purified human apurinic/apyrimidinic endonuclease-1 (APE1) and APE1 from human cell extracts efficiently process an rAP site in DNA and have weak endoribonuclease and 3′-exonuclease activities on r8oxoG substrate. Using biochemical assays, our results provide evidence of a human enzyme able to recognize and process abasic and oxidized ribonucleotides embedded in DNA.

INTRODUCTION

Incorporation of ribonucleotides monophosphate (rNMPs) in DNA is a frequent phenomenon, which is considered the most common type of 'DNA damage' occurring in normal cells (1,2). Ribose-seq and other approaches recently developed for mapping sites of rNMPs in DNA have shown widespread but not random distribution of rNMPs in chromosomal DNA of budding and fission yeast (2) (and references therein). The number of rNMPs identified per nuclear chromosome was found to be proportional to chromosome size (2), and quantitation approaches have estimated a 600,000 rNMPs in budding yeast genome and over 100 millions in mouse genome (3).

The incorporation of rNMPs in genomic DNA may be due to: (i) the disequilibrium in the cellular pool of deoxyribonucleotides (dNTPs) and ribonucleotides (rNTPs) (2), (ii) an incomplete elimination of RNA primers used in the generation of Okazaki fragments (4), (iii) an oxidation of the deoxyribose sugar into ribose (5) and last but not least, (iv) an imprecise 3′-exonucleolytic proofreading activity of replicative DNA polymerases, which do not discriminate rNMPs from dNMPs pool (2,4,6,7). Furthermore, taking into consideration all rNMPs that are synthesized during lagging strand synthesis, more than 100 million rNMPs are introduced into the mammalian genome per cell cycle (3). In addition, it has been estimated that the amount of rNTPs is generally 40–350-fold higher than that of dNTPs in cycling cells (6–8) increasing the probability of incorrect rNMP incorporation during DNA replication and repair (2,4,6,7).

The effects of the 2′-hydroxyl group of the ribose sugar within an rNMP embedded in DNA are numerous: it mainly alters DNA elasticity and structure in a sequence dependent manner (9–11) and affects the activity and function of several DNA-interacting proteins, in addition to increase the DNA fragility and mutability (1,12). Moreover, rNMPs in DNA can be template for DNA synthesis (13,14), although the DNA polymerases processivity on rNMP tracts is reduced (13).

*To whom correspondence should be addressed. Email: gianluca.tell@uniud.it and storici@gatech.edu
†These authors contributed equally to this work as first authors.

The main pathway deputed to rNMPs removal is ribonucleotide excision repair (RER), in which the principal enzyme is RNase H2. It was demonstrated that RNase H2 deficiency in mammalian cells is associated to DNA damage repair activation and, in humans, to pathology. RNase H2-null murine embryonic fibroblasts (MEFs) activate a p53-dependent damage response, whereas null-RNase H2 are embryonic lethal (15). In humans, mutations in each of the three subunits of RNase H2 are associated with the neurological syndrome of Aicardi-Goutières (AGS), which causes severe brain dysfunction (16–18). Altered RNase H2 function in AGS patients may result in increased level of rNMPs in DNA, which could in turn activate DNA damage response signaling and induce innate immune response (19,20).

Besides RER, other different DNA repair mechanisms are active to remove rNMPs embedded in DNA (3,21). In the absence of RNase H2, topoisomerase I cleavage (21), followed by nick processing by Srs2–Exo1, can remove some rNMPs (22,23). rNMPs in DNA can be also targeted by the nucleotide excision repair (NER) factors in bacteria (24). However, *in vitro* experiments showed that human NER proteins are not active to remove rNMPs embedded in DNA (25). Differently, the mismatch repair (MMR) mechanism targets mismatches with rNMPs both in *Escherichia coli* and *Saccharomyces cerevisiae* genomic DNA (26). Until now, there is no proof that the base excision repair (BER) mechanism plays any role in removing rNMPs from DNA.

BER is known to repair a wide spectrum of oxidative lesions in nuclear and mitochondrial DNA (27,28), and preventing cancer (29,30). Abasic sites, which form by spontaneous hydrolysis of the N-glycosidic bond in DNA or following removal of a damaged base by BER glycosylases, are major targets or intermediate substrates in the BER pathway of DNA repair (31). It has been estimated that up to 10,000 abasic sites are formed per human genome per day (32). Despite the fact that spontaneous depurination occurs ∼1,000 times slower in RNA than DNA (33), due to the high abundance of rNMPs in genomes, with >100 million rNMPs transiently present in mammalian DNA during one replication cycle, considering rNMP incorporation by DNA polymerases during DNA replication and repair, and RNA primers of Okazaki fragments (3), the possibility that abasic and oxidized rNMPs (such as 7,8-dihydro-8-oxoriboguanosine) are present in DNA and are targets of BER is quite real and worth careful study. These data, together with other recent findings about the ability of *Schizosaccharomyces pombe* Pol 4, *Mycobacterium smegmatis* DinB2 and human Polβ to insert and elongate oxidized rGMP when paired with dA during DNA replication (34–36), underscore the necessity to determine how cells can target and remove oxidized rNMPs or rAP sites from DNA.

Because recent studies point toward a new function of BER in RNA surveillance (37,38), there is high likelihood that BER could be involved in the processing of rNMPs in DNA, particularly in the case of chemically modified rNMPs, such as abasic and oxidized rNMPs. Identifying whether BER may target normal and modified rNMPs in DNA is important to better understanding the mechanism of genotoxicity of reactive oxygen species, the function and the impact of BER defects in human disease and cancer mechanisms. In the absence of proper repair mechanisms to cope with these kind of lesions, even a single or a few modified rNMPs present in a genome per cell cycle could lead to mutations and/or genomic rearrangements.

Findings from our and other laboratories have revealed an important involvement of the apurinic/apyrimidinic endonuclease 1 (APE1) in RNA metabolism and RNA-decay (37–40). APE1 is by far one of the most studied enzymes in the BER pathway for its altered expression in different human pathologies ranging from neurodegenerative to cancer disorders (41). Its role in DNA repair is primarily due to its ability to act as an endonuclease, specifically able to cleave 5′ to deoxy- abasic sites, which results in a strand break with 3′-hydroxyl and 5′-phosphodeoxyribose termini. APE1 also has redox activity needed to modulate the DNA binding ability of several transcription factors (41). As recently demonstrated, APE1 can endonucleolytically cleave abasic single-stranded RNA (37,38,40), has a 3′-RNA phosphatase activity, and a weak 3′-5′ exoribonuclease activity (42). Moreover, it has been demonstrated that APE1 has nucleotide incision repair (NIR) activity on modified bases, such as 5,6-dihydro-2′-deoxyuridine, 5,6-dihydrothymidine, 5-hydroxy-2′-deoxyuridine, 5-hydroxycytosine, which are directly repaired by APE1 bypassing the action of specific glycosylases (43–45). Therefore, we hypothesized that APE1 can be involved in processing rNMPs in DNA, particularly in the case of abasic and oxidized rNMPs.

Here, we found that eukaryotic RNase H2 from yeast, mouse and human is inactive on an rAP site in DNA in different assays. We discovered and characterized an unknown APE1 activity on abasic ribonucleotide embedded in DNA. We then compared the ability of human RNase H2 to cleave at an oxidized ribonucleotide (r8oxoG) incorporated in a DNA substrate and analyzed the activities of 8-oxoguanine DNA glycosylase (OGG1) and APE1 to recognize and cleave this particular type of damage. Our data demonstrate that APE1, but not human RNase H2 and OGG1, has a weak endoribonuclease activity on the oxidized substrate.

MATERIALS AND METHODS

Double strand synthetic oligonucleotides description and annealing conditions

All oligonucleotides and their complementary sequences used in this study are listed in Supplementary Table S1 (see also Supplementary Figure S1). ss_dG_40 oligonucleotide and its reverse complementary sequence, ss_dC_40, were purchased from Invitrogen (Grand Island, NY, USA). ss_rG_40 oligonucleotide and the DNA oligo containing a tetrahydrofuran abasic deoxyribonucleotide, ss_dF_40, or tetrahydrofuran abasic ribonucleotide, ss_rF_40, as well as ribo- 1′OH abasic containing oligonucleotide, ss_rOH, were purchased from Dharmacon (GE Healthcare, Lafayette, CO, USA). The 26-mer oligonucleotide containing a tetrahydrofuran, ss_dF, and its reverse complementary sequence ss_dC, were synthesized from Metabion International AG (Steinkirchen, Germany). The 25-mer dG-, rG-, d8oxoG-containing oligonucleotides and complementary oligonucleotides were synthesized from Metabion International AG (Steinkirchen, Germany).

ss_dG_40, ss_rG_40, ss_dF_40 and ss_rF_40 oligonucleotides were 5′ end-labeled with [γ-^{32}P] ATP (PerkinElmer, Boston, MA, USA) by T4 polynucleotide kinase (PNK) (New England BioLabs, Ipswich, MA, USA) in a reaction mixture containing 10 μM ATP using 10X PNK buffer (New England BioLabs, Ipswich, MA, USA). This labeling reaction was incubated at 37°C for 1 h, followed by inactivation at 65°C for 20 min. The reactions were purified by using Illustra MicroSpin G-25 column (GE Healthcare, Buckinghamshire, UK).

The remaining oligonucleotides were labelled with either IRDye700, IRDye800 fluorophores or Cyanine5 at 5′ end, as specified in Supplementary Table S1, purified through RP-HPLC, checked in Mass Check and re-suspended in RNase- and DNase- free water.

Synthesis of oligonucleotide containing an internal ribose 8-oxo-guanosine (r8oxoG) and an IRDye700 fluorophore at 5′ end was in-house carried out on an Applied Biosystems 392 DNA/RNA synthesizer using the phosphoramidite chemistry, associated with the phenoxyacetyl protecting group for the nucleobases and the *tertio*-butyldimethylsilyle protecting group at the 2′-OH position of the ribonucleoside residue (46). Upon completion, the oligonucleotide was de-protected in concentrated aqueous ammonia for 6 h at 55°C, followed by a desilylation step with triethylamine trihydrofluoride (8 h at room temperature) (46) and was finally purified by preparative 20% denaturing PAGE using UV-shadowing detection. After desalting by size exclusion, the r8oxoG oligonucleotide was quantified by UV measurements at 260 nm and its purity was checked by RP-HPLC analysis together with MALDI-TOF mass measurements (Supplementary Figure S5, panels A and B). Sample was then lyophilized and frozen at –20°C until use.

All oligonucleotides used in the present study were re-suspended in RNase- and DNase-free water at 100 μM. 100 pmol of each oligonucleotide was annealed with an excess of 150 pmol of its complementary DNA oligonucleotide (as indicated in Supplementary Table S1) in 10 mM Tris–HCl pH 7.4 and 10 mM $MgCl_2$, heated at 95°C and cooling down over night in the dark.

Plasmid and expression of recombinant proteins

Plasmids and expression of human recombinant OGG1 enzyme was purified as described by Audebert *et al*. (47). Plasmids and expression of human recombinant APE1 wild type (WT) and respective mutants (APE1 NΔ33 and APE1 E96A) were produced as explained by Fantini *et al.* (48) and Erzberger and Wilson (49). Plasmid and expression of yeast, mouse and human recombinant RNase H2 were produced as explained by Chon *et al.* (50,51).

Cell lines and silencing experiments

HeLa cells (human cervical carcinoma) (ATCC®, Milan, Italy) were grown in DMEM (EuroClone, Milan, Italy) supplemented with 10% fetal bovin serum (FBS-EuroClone, Milan, Italy), penicillin (100 U/ml), streptomycin (100 mg/ml) and L-glutamine (2 mM) (EuroClone, Milan, Italy) and cultured in a humidified incubator at 5% CO_2 at 37°C.

For silencing experiments, 15×10^4 cells were seeded and transfected with 5′ UACUCCAGUCGUACCAGACCU 3′ siAPE1 (100 pmol) or siGENOME SMART pool siRNase H2A (50 pmol) or 5′ CCA UGA GGU CAG CAU GGU CUG UU 3′ scramble control siRNA (100 pmol) (GE Dharmacon, Milan, Italy) by using Oligofectamine™ Reagent (GE Dharmacon, Milan, Italy) as per manufacturer's indications. After 72 h upon transfection, cells were harvested by trypsinization and centrifuged at 250 × g for 5 min at 4°C. Supernatant was removed, and pellet was washed once with ice-cold phosphate-buffered saline without Calcium and Magnesium (PBS-Euroclone, Milan, Italy) and then centrifuged again (250 × g for 5 min at 4°C).

Preparation of nuclear cell extracts (NCE)

After washing with PBS, cells were collected in cold PBS added with 0.1 M DTT and 0.5 mM phenylmethylsulfonyl fluoride (PMSF). Cells were centrifuged at 800 × g for 10 min at 4°C and the supernatant was removed. Pellet was re-suspended in a cold hypotonic solution containing 10 mM HEPES pH 7.9, 10 mM KCl, 0.1 mM $MgCl_2$, 0.1 mM EDTA pH 8.0 complemented with 0.1 mM DTT, 0.5 mM PMSF, 1 mM protease inhibitor (PI), 1 mM NaF, 1 mM Na_3VO_4. After centrifugation at 800 × g for 10 min at 4°C, cytosolic proteins (CCE) were collected whereas intact nuclei were pelleted. Pellet was washed to discard any contamination from cytosol and it was subsequently re-suspended with a cold hypertonic solution 20 mM HEPES pH 7.9, 420 mM NaCl, 1.5 mM $MgCl_2$, 0.1 mM EDTA pH 8.0, 5% glycerol complemented with 0.1 mM DTT, 0.5 mM PMSF, 1 mM PI, 1 mM NaF, 1 mM Na_3VO_4 and incubated on ice for 30 min. At the end, the sample was centrifuged at 15,000 × g for 20 min at 4°C and collected the supernatant containing nuclear proteins (NCE). Quantification of each sample was performed by colorimetric Bradford assays (Bio-Rad, Milan, Italy).

Preparation of whole cell extracts (WCE)

After washing with PBS, cells were harvested by trypsinization and centrifuged at 250 × g for 5 min at 4°C. The supernatant was removed, washed once with PBS and centrifuged again. Pellet was re-suspended in a lysis solution containing 50 mM Tris–HCl (pH 7.4), 150 mM NaCl, 1 mM EDTA, 1% (w/v) Triton X-100 supplemented with 1 mM PI, 1 mM DTT, 0.5 mM PMSF, 1 mM NaF and 1 mM Na_3VO_4. After centrifugation at 15 000 × g for 20 min at 4°C, the supernatant is considered as whole cell extract (WCE). Proteins of each sample were quantified using a colorimetric Bradford assays (Bio-Rad, Milan, Italy).

Enzymatic activity assays

To measure enzymatic activity of recombinant proteins and NCE on different substrates, each reaction was prepared following doses, time points and buffers specified in detail into the legend of each experiment. Final volume for each reaction was 10 μl. At the end of all reactions, samples were blocked with a stop solution, containing 99.5% (v/v) formamide (Sigma-Aldrich, Milan, Italy) supplemented with

10× Orange Loading Dye (Li-Cor Biosciences, Milan, Italy) and heated at 95°C for 5 min. Then, all samples were loaded onto a 7 M denaturing 20% polyacrylamide gel in TBE buffer pH 8.0 and run at 4°C at 300 V for 1 h. Then, the gel was visualized with an Odyssey CLx Infrared Imaging system (LI-COR GmbH, Germany). The signals of the non-incised substrate (S) and the incision product (P) bands were quantified using Image Studio software (LI-COR GmbH, Germany). When using the ds_rOH:dC and ds_r8oxoG:dC oligonucleotides, a very small amount of cleavage product was seen in samples not treated with recombinant proteins and/or cell extracts due to the reactivity of this molecule, which was spontaneously degraded. During the analysis, this band has been always subtracted from bands obtained following treatment with recombinant proteins and/or extracts.

For radioactive experiments, reactions were stopped by adding 2× denaturing PAGE gel buffer (0.01% bromophenol blue, 95% formamide and 20 mM EDTA pH 8.0) and heating to 95°C for 5 min. After dilutions, the products were analyzed by 15% (w/v) polyacrylamide, 8 M urea gel electrophoresis (urea–PAGE). 20–100 Oligonucleotide Length Standard (Integrated Device Technology, Coralville, IA, USA) was used as a ladder (M). After electrophoresis, gels were exposed to phosphor screen overnight. Images were taken with Typhoon Trio+ (GE Healthcare, Lafayette, CO, USA) and obtained with ImageQuant (GE Healthcare). Band intensities were quantified by Multi Gauge V3.0 (Fujifilm).

Electrophoretic mobility shift assay analysis (EMSA)

Proteins binding to nucleic acids was assessed by EMSA analysis as already described by Fantini *et al*. (48). Briefly, the indicated amounts of recombinant purified proteins or cell extracts were co-incubated with 250 fmol of the probe (25 nM) at 37°C for 30 min. Reactions were prepared in a buffer containing 8 mM HEPES, 10 mM KCl, 400 μM EDTA pH 8.0, 5 mM DTT and 2% glycerol in a 10 μl final volume. Moreover, salmon sperm DNA (SSD) (Sigma-Aldrich, Milan, Italy) was added like as DNA competitor. Samples were loaded onto an 8% (w/v) native polyacrylamide gel in tris-sodium acetate–EDTA pH 8.0 (TAE) buffer and run at 4°C at 150 V for 1 h followed by 3 hat 250 V.

Statistical analysis

Statistical analyses were performed by using the Student's *t* test. $P < 0.05$ was considered as statistically significant.

RESULTS

Human, yeast or mouse RNase H2 does not process an rAP site embedded in DNA

RNase H2 is the principal protein able to process paired and mismatched rNMP sites embedded in DNA by generating a nick to their 5′ side (26) (and references therein). Up to now, whether RNase H2 can cleave an rAP site incorporated in a duplex DNA is unknown. In order to test this hypothesis, we measured RNase H2 ability to cleave a modified

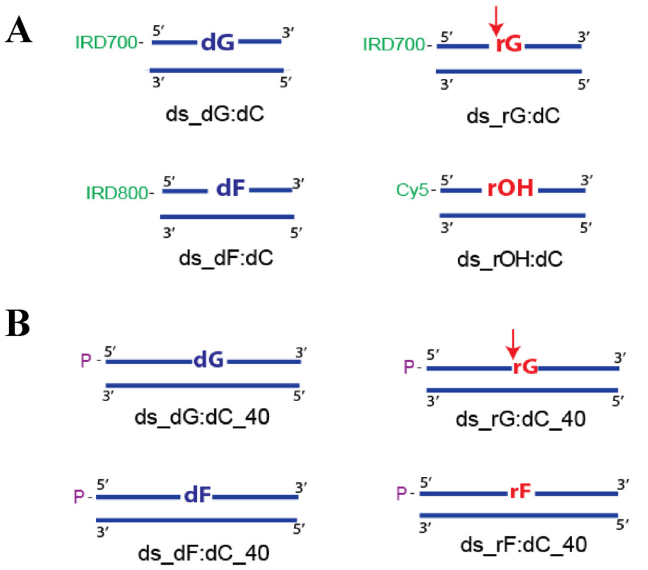

Figure 1. Scheme of substrates used to test cleavage of an rAP site in DNA. DNA nucleotides are in blue, RNA in red. The 5′ and 3′ ends of each DNA strand are indicated. (**A**) Scheme of double strand (ds) DNA 25-mer substrates (single strand (ss) oligonucleotide annealed to ss_dC containing-complementary oligonucleotide) containing a dGMP, rGMP, dF and 1′ OH abasic rNMP (rOH) site in the 13th position. The 'IRD700' in green indicate IRDye 700 phosphoramidite dye tagged at the 5′ end. The 'IRD800' in green indicate IRDye 800 phosphoramidite dye tagged at the 5′ end. The 'Cy5' in green indicates cyanine dye tagged at the 5′-end of the top strand of the duplex. (**B**) Scheme of the ds_DNA 40-mer substrate (ss oligonucleotide annealed to its ss complementary oligonucleotide) containing a dGMP, rGMP, dF and rF site in the 20th position. The P in purple indicates radiolabelled ^{32}P at the 5′-end of the top strand of the duplex. The red arrow indicates the cleavage position by RNase H2 5′ to the rGMP site.

25-mer DNA oligonucleotide, called ds_rOH:dC, in which a 1′-OH abasic rNMP was incorporated into a DNA substrate as shown in Figure 1A (see also Supplementary Table S1 and Supplementary Figure S1). First of all, recombinant human RNase H2, composed of its three subunits, was purified as explained in Materials and Methods (Supplementary Figure S2) and its activity was tested on ds_rOH:dC oligonucleotide in parallel with dG- and rG- containing oligonucleotides as negative and positive controls, respectively. As reported in Figure 2, the enzyme had no activity on ds_dG:dC and ds_dF:dC (containing a tetrahydrofuran residue mimicking the abasic site) oligonucleotides, whereas it efficiently cleaved the canonical rG substrate as expected. In addition, we tested the mismatched rG- containing oligonucleotide, ds_rG:dA, confirming that RNase H2 protein is also active on this type of substrate (Figure 2A). On the other hand, no activity was detectable on ds_rOH:dC demonstrating that recombinant human RNase H2 is not able to process an abasic rNMP embedded in DNA. To confirm these data in cells, we tested the activity of RNase H2 protein obtained from nuclear cell extracts on the same substrates, as above (Figure 2). To this aim, RNase H2 expression was downregulated in HeLa cells through specific siRNA and the endoribonuclease activities of nuclear extracts from knocked down and control cells were then assayed. Western blotting analyses performed on nuclear extracts from control (Scramble) and knocked down

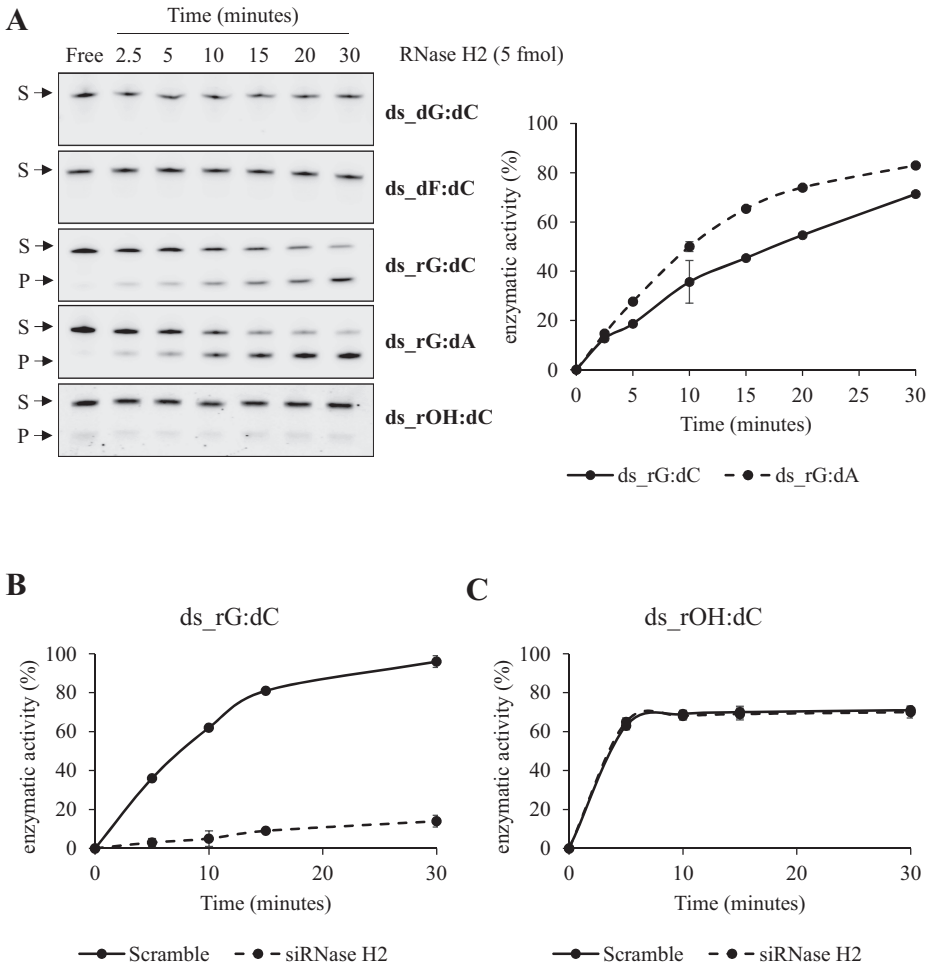

Figure 2. Human RNase H2 is not able to process an rAP site embedded in a duplex DNA substrate. (**A**) Representative denaturing polyacrylamide gel of oligonucleotides (25 nM) incision by recombinant human RNase H2 (0.5 nM). The reaction was performed in RNase H2-buffer (20 mM Tris–HCl, 25 mM KCl, 0.1% BSA, 0.01% Tween20, 4 mM $MgCl_2$, pH 7.4) for different time points, expressed in minutes and shown on the top of the figure, at 37°C. ds_dG:dC and ds_dF:dC oligonucleotides were used as negative controls whereas paired and mismatched ds_rG oligonucleotides as positive controls. S indicates the substrate position while P indicates the product position (*left*). Relative graph illustrating the time-course kinetics activity of the recombinant protein on ds_rG:dC and ds_rG:dA oligonucleotides. Data are expressed as mean ± SD of three independent technical replicas (*right*). (**B**) Graph illustrating the time-course kinetics activity of NCE on ds_rG:dC in control and RNase H2-knocked down conditions. Enzymatic reaction was performed at 37°C in RNase H2-buffer with 500 ng of NCE. Data are expressed as mean ± SD of three independent technical replicas. Standard deviation values were always less than 10% of the mean of the experimental points. (**C**) Graph illustrating the time-course kinetics activity of NCE on ds_rOH:dC oligonucleotide in control and RNase H2-knocked down conditions. Enzymatic reaction was performed at 37°C in RNase H2-buffer with 500 ng of NCE. Data are expressed as mean ± SD of three independent technical replicas. Standard deviation values were always less than 10% of the mean of the experimental points.

(siRNase H2) cells demonstrated the efficiency of RNase H2 downregulation (∼50%) upon transfection with specific siRNA sequences (Supplementary Figure S3A). We incubated Scramble or siRNase H2 cell extracts with different substrates for the indicated time points. Following knock-down of RNase H2, we found a decreased cleavage of ds_rG:dC, as expected (Figure 2B and Supplementary Figure S3B). Surprisingly, we found that ds_rOH:dC was also cleaved; however, ds_rOH:dC cleavage was completely unaffected by siRNase H2 cell extracts (Figure 2C and Supplementary Figure S3B). These data suggest that while human RNase H2 is inactive on an abasic rNMP embedded in DNA, there is another enzyme/s capable of cleaving it in human cells.

To increase the stability of the abasic rNMP-containing oligonucleotide, we also used abasic substrates mimicked by tetrahydrofuran (F) residues, similarly to what commonly used for dNMP (52,53). We then tested whether RNase H2 from yeast or mouse may process an abasic rNMP, mimicked by a tetrahydrofuran ribonucleotide residue, embedded in a longer DNA sequence composed of 40-bp to evaluate a possible role of the length of the substrate in determining the inability of RNase H2 to process these substrates (Figure 1B). We used single-stranded (ss) or double-stranded (ds) DNA substrates containing an abasic rNMP site (rF), an rGMP (rG), an abasic dNMP (dF) or a dGMP as internal controls (Supplementary Table S1). As expected, *S. cerevisiae* and mouse RNase H2 cleaved at the single rG in a DNA duplex substrate (*lane 9* in Figure 3, panels A and B, respectively) and had no activity on the rG embedded in the ss substrate (*lanes 7* and *8* in Figure 3, panels A and B). Importantly, as we found for human RNase H2, also *S.*

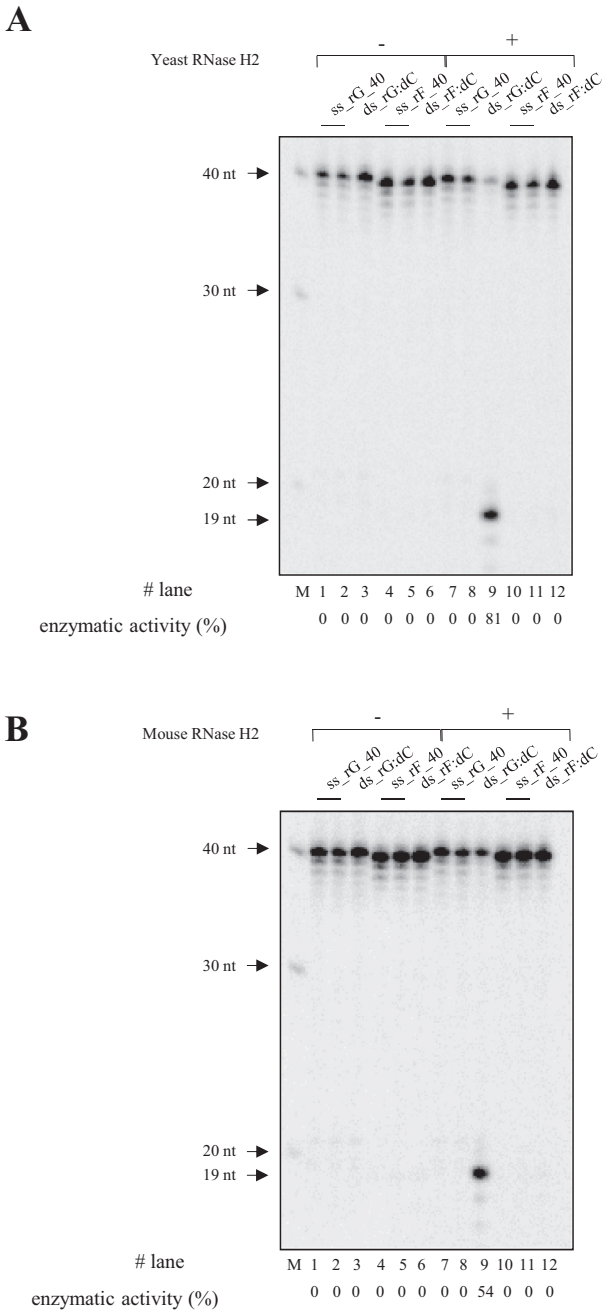

Figure 3. Mouse and yeast RNase H2 are not able to process an rAP site embedded in a duplex DNA substrate. (A and B) Denaturing PAGE gels showing cleavage result using 10 nM of 40-mer radioactive substrate containing an rG or an rF site, without (*lanes 1–6*) or with (*lanes 7–12*) 10 nM of yeast RNase H2 protein (**A**) or 10 nM of mouse RNase H2 protein (**B**). All reactions were carried out at 37°C for 1 h in yeast/mouse reaction 1× buffer (15 mM Tris–HCl pH 8.0, 50 mM NaCl, 10 mM $MgCl_2$, 5% glycerol, 1 mM DTT and 0.1 mg/mL BSA). M indicates the DNA ladder and the black arrows on the left of each panel show specific band sizes. *Lanes 1,7* have ss-substrate containing rG (ss_rG_40), *lanes 2,8* have ss-substrate containing ss_rG_40 that is cooled slowly at room temperature to demonstrate the absence of any self-annealing structures, and *lanes 3,9* show the ds-substrate containing rG (ds_rG_dC). *Lanes 4,10* have ss-substrate containing abasic ribo site (ss_rF_40), *lanes 5,11* have ss_rF_40 that is cooled slowly in room temperature to observe any self-annealing; and *lanes 6,12* have ds substrate containing abasic ribo site (ds_rF:dC). The percentages of cleavage of each reaction are displayed below the images as enzymatic activity (%).

cerevisiae and mouse RNase H2 complexes were inactive on the abasic rNMP, ds_rF:dC (*lane 12* in Figure 3, panels A and B). Together these results demonstrate the inability of eukaryotic RNase H2, both from yeast and mammalian origins, to process an abasic rNMP incorporated in DNA independently from the nature of the abasic site (either 1′-OH or tetrahydrofuran residue) and the length of the substrate (either 25- or 40-mers).

Human APE1 is able to process an rAP site embedded in DNA through its endonuclease catalytic domain

To test the ability of APE1 to process rAP sites in DNA, we purified human recombinant APE1 protein, as described in Materials and Methods section (Supplementary Figure S4A). The endonuclease activity of APE1 on ds_rOH:dC substrate was examined through cleavage assays. As a positive control for APE1 endonuclease activity, an oligonucleotide substrate containing a tetrahydrofuran residue mimicking the abasic site, called ds_dF:dC (52,53), was used. As reported in Figure 4A, and measured through kinetics experiments in Table 1, APE1 processes the abasic rNMP as efficiently as the canonical deoxyabasic site having a lower affinity for the ds_rOH:dC than the ds_dF:dC (11-fold increase of the K_M) but a higher catalytic rate (27-fold increase in the k_{cat}/K_M ratio) (Table 1). Moreover, APE1 was unable to process the rG- containing oligonucleotide, which is the preferential substrate of RNase H2 enzyme. To further characterize the enzymatic activity of APE1, we used the purified recombinant mutant APE1 E96A protein, in which the missense mutation of the residue in the catalytic site, characterized by the substitution of the glutamic acid in position 96 with alanine, causes a decreased enzymatic activity of the protein, lacking the ability to coordinate the Mg^{2+} ion in the catalytic site (52,54,55) (Supplementary Figure S4B). In addition, we used the purified recombinant mutant APE1 NΔ33 protein, in which the first 33 N-terminal residues, responsible for RNA-protein interaction but not affecting its enzymatic activity, have been deleted (32,38) (Supplementary Figure S4B). Following incubation of ds_rOH:dC with APE1 E96A mutant, there was barely any endonuclease activity, whereas the activity of APE1 NΔ33 mutant was comparable with that of the APE1 WT protein (Figure 4, panels B and C and Supplementary Figure S4C). These data demonstrate that the catalytic domain of APE1 is responsible for recognizing and cleaving a rAP site in dsDNA and that the N-terminal domain does not play any major role in the enzymatic activity on this substrate and that AP endonucleolytic activity on rAP sites is intrinsic to the purified protein.

Kinetic parameters (K_M, V_{MAX} and k_{CAT}) were calculated from the measurement of the endonucleolytic reaction rates for APE1 on ds_dF:dC and ds_rOH:dC substrates. As described by Fantini *et al.* (48), increasing concentrations of the substrate were incubated with a selecting concentration of the protein (see first column) in a time-course experiment. Kinetic values were calculated using a Lineweaver–Burk plot analysis and represent the mean ± SD of three independent experiments.

To confirm that APE1 is the major enzyme capable of cleaving ribo-abasic containing sites in cells, we used

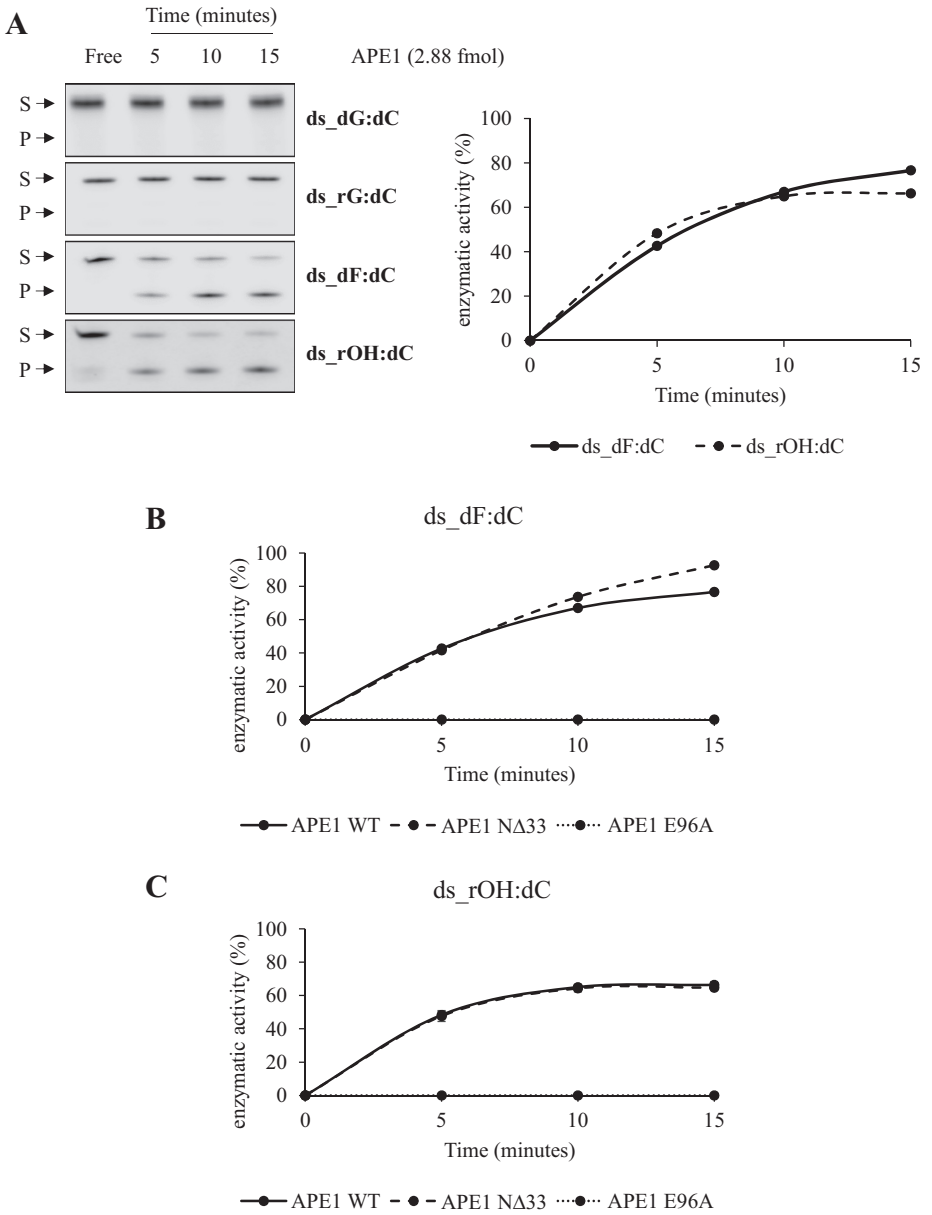

Figure 4. Human APE1 efficiently processes an rAP site embedded in a duplex DNA substrate. (**A**) Representative denaturing polyacrylamide gel of oligonucleotides (0.25 μM) incision by recombinant human APE1 (0.288 nM). The reaction was performed in APE1-buffer (20 mM Tris–HCl, 100 mM KCl, 0.1% BSA, 0.01% Tween20, pH 7.4) for different time points, expressed in minutes and shown on the top of the figure, at 37°C. ds_dG:dC and ds_rG:dC oligonucleotides were used as negative controls, whereas ds_dF:dC oligonucleotide as positive control. S indicates the substrate position, while P indicates the product position (*left*). Relative graph illustrating the time-course kinetics activity of the recombinant protein on ds_dF:dC and ds_rOH:dC oligonucleotides. Data are expressed as mean ± SD of three independent technical replicas. Standard deviation values were always <10% of the mean of the experimental points (*right*). (**B**) Graph illustrating the time-course kinetics activity of APE1 mutants on ds_dF:dC oligonucleotide. Data are expressed as mean ± SD of three independent technical replicas. Standard deviation values were always <10% of the mean of the experimental points. (**C**) Graph illustrating the time-course kinetics activity of APE1 mutants on ds_rOH:dC oligonucleotide. Data are expressed as mean ± SD of three independent technical replicas. Standard deviation values were always <10% of the mean of the experimental points.

Table 1. Kinetic parameters for APE1 endonuclease activity on different substrates

[APE1] ($\times 10^{-3}$ nM)	Substrate	K_M (nM)	V_{MAX} (nM/min)	k_{CAT} (min^{-1})	k_{CAT}/K_M $(min.nM)^{-1}$
75	ds_dF:dC	14.2±6.98	0.95±0.33	12.7±4.39	0.95±0.16
3.125	ds_rOH:dC	158±41.79	12.66±3.71	4054±1191.8	26±1.96

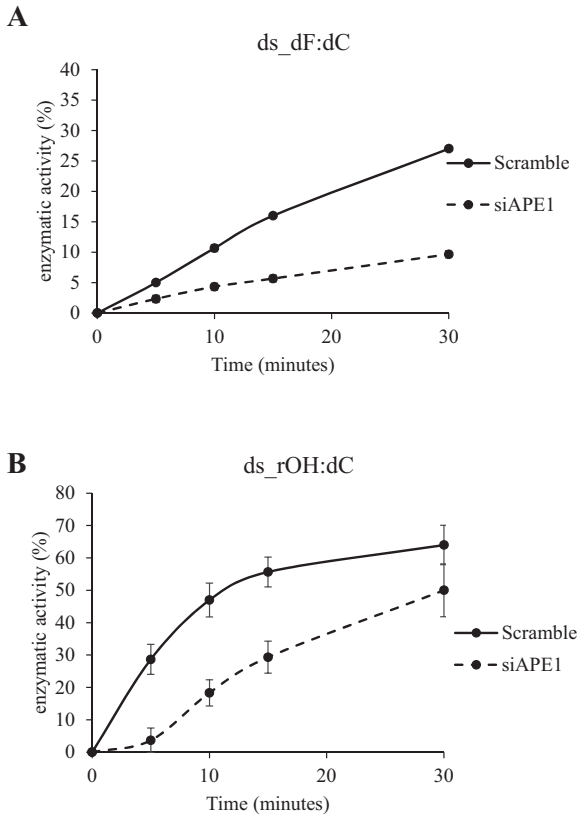

Figure 5. APE1 knock down in human cells impairs the processing of an rAP site embedded in a duplex DNA substrate. (**A**) Graph illustrating the time-course kinetics activity of NCE on ds_dF:dC in control and APE1-knocked down conditions. Data are expressed as mean ± SD of three independent technical replicas. Standard deviation values were always less than 10% of the mean of the experimental points. (**B**) Graph illustrating the time-course kinetics activity of NCE on ds_rOH:dC oligonucleotide in control and APE1-knocked down conditions. Enzymatic reaction was performed at 37°C in APE1-buffer with 10 ng of NCE. Data are expressed as mean ± SD of three independent technical replicas.

nuclear cell extracts in which APE1 was knocked-down through specific siRNAs (Supplementary Figure S3A), as explained in Materials and Methods. The endonuclease activity of APE1-kd (siAPE1) cell extracts, was reduced on both ds_dF:dC (Figure 5A and Supplementary S4D) and ds_rOH:dC (Figure 5B and Supplementary S4D), as compared to its respective control SCR-treated extracts. As western blot analysis shows (Supplementary Figure S3A), the expression of APE1 protein did not exert any effect on the expression of RNase H2 protein itself, demonstrating that the observed reduction of the processing activity of the abasic rNMP-containing substrate, observed with APE1-kd cell extracts, was likely due to the reduced expression of the APE1 protein. We further examined the specificity of the enzymatic activity of APE1 using the tetrahydrofuran ribonucleotide mimicking an abasic residue. We tested the activity of the APE1 E96A mutant to cleave at a ds_rF:dC substrate compared to that of APE1 WT (Figure 6A). As a control, the activity on the ds_dF:dC substrate was also analyzed. As it can be observed, mutant E96A showed a reduced cleavage on the ds_rF:dC substrate. Indeed, APE1 WT gave a 96% of cleavage at 5 and 10 nM (*lanes 2 and 3*), whereas mutant APE1 E96A had 32% cleavage at 5 nM and 38% at 10 nM (*lanes 5 and 6*). Cleavage of ds_rF:dC by APE1 WT was 89% at 5 nM and 90% at 10 nM (*lanes 8 and 9*), and there was minimal activity for APE1 E96A on the ds_rF:dC substrate in the same conditions (*lanes 11 and 12*). Moreover, pre-treatment of cell extracts with 0.2 nM of Compound #3 (i.e. *N*-(3-(benzo[d]thiazol-2-yl)-6-isopropyl-4,5,6,7-tetrahydrothieno[2,3-c]pyridin-2-yl)acetamide)), a specific APE1 endonuclease inhibitor (53,56), exerted a significant inhibitory effect upon APE1 enzymatic activity on both ds_dF:dC in DNA and ds_rF:dC substrates demonstrating that the main enzymatic activity of cell extracts was due to APE1 function (Figure 6, panels B and C).These data demonstrate that human APE1 is the major enzyme capable of specifically cleaving at abasic rNMPs in DNA while being unable to process normal rNMPs, which are the preferential substrates of RNase H2.

Human RNase H2 does not process an r8oxoG embedded in a duplex DNA

An abasic site can be generated spontaneously or following the processing of an oxidized lesion from a specific glycosylase. While known glycosylases (such as OGG1) are responsible for this activity on 8oxo-dG, no enzyme is known to be able to process the oxidized rG substrate. We then focused our attention on r8oxoG removal. The r8oxoG containing oligonucleotide was in-house synthesized and, as observed from MALDI-MS analysis and HPLC purification (Supplementary Figure S5, panels A and B), the undesirable presence of secondary products of the chemical synthesis of this substrate can be excluded. First of all, we investigated whether human RNase H2 was able to recognize and cleave at r8oxoG site using an oligonucleotide containing this type of lesion called ds_r8oxoG:dC (Figure 7A, see also Supplementary Table S1, Supplementary Figure S1). In these experiments, we always compared the specific enzymatic activity of RNase H2 with that exerted on the canonical ds_rG:dC substrate, as positive control, and using the ds_d8oxoG:dC oligonucleotide as negative control. As Figure 7B shows, while the ds_rG:dC oligonucleotide was efficiently processed by RNase H2, the same activity was not observed for ds_r8oxoG:dC. As expected, the d8oxoG-containing oligonucleotide was not cleaved by RNase H2. These data confirm that RNase H2 was not able to process modified rNMPs embedded in DNA. Similarly, we confirmed these data using RNase H2-kd nuclear extracts from HeLa cells. As expected, control nuclear extracts (Scramble) displayed a time-dependent endoribonuclease activity on ds_rG:dC, whereas the down regulation of RNase H2 protein expression (siRNase H2) was associated with a marked reduction of the endoribonuclease activity on the same substrate (Figure 7C). On the contrary, once we tested the ability of the nuclear extracts on ds_r8oxoG:dC oligonucleotide, we found only a weak endoribonuclease activity on it (see the band indicated by an asterisk), which was not affected by RNase H2 silencing (Figure 7C). These data support the conclusion that the r8oxoG site in DNA is not recognized by human RNase H2.

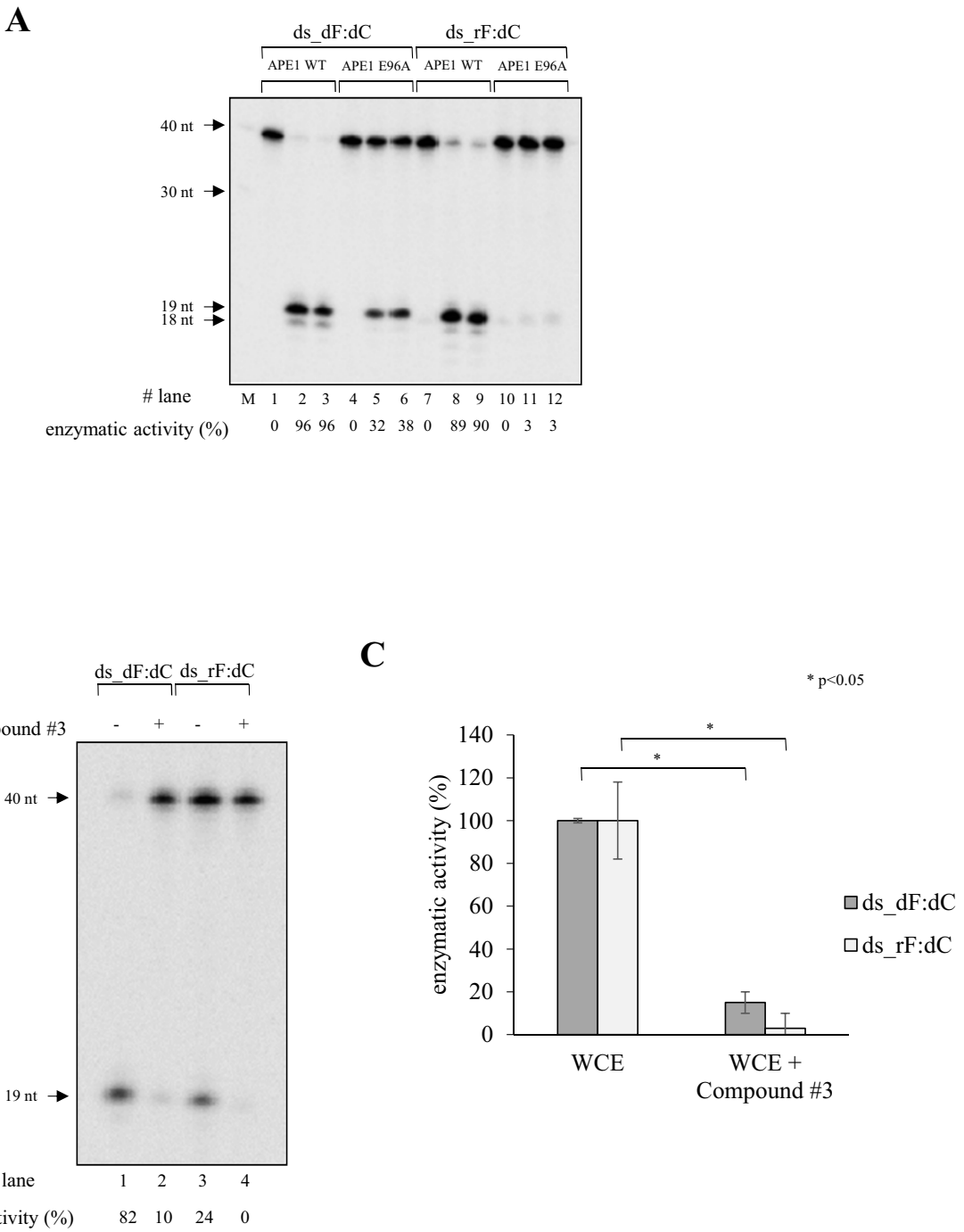

Figure 6. Recombinant human APE1 efficiently processes a tetrahydrofuran ribonucleotide mimicking an abasic residue site (rF) embedded in a duplex DNA substrate. (**A**) Cleavage result of 10 nM of ^{32}P double-stranded oligonucleotides ds_dF:dC or ds_rF:dC substrates with different concentrations of APE1 WT protein (*lanes 1–3* and *7–9*) and mutant APE1 E96A protein (lanes *4–6* and *10–12*) at 37°C for 1 h in APE1-reaction 1× buffer containing 50 mM Tris–HCl pH 7.5, 50 mM KCl, 10 mM $MgCl_2$, 0.001 mg/mL BSA and 0.05% Triton X-100. First lane on the left, M is a ssDNA ladder (barely visible) and the black arrows on the left show specific band sizes. Both oligonucleotides were incubated with 0 nM (*lanes 1,4,7,10*), 5 nM (*lanes 2,5,8,11*) or 10 nM (*lanes 3,6,9,12*) of APE1 WT protein (*lanes 1–3* and *7–9*) or mutant E96A protein (*lanes 4–6* and *10–12*), respectively. The percentages of cleavage of each reaction are displayed below the image as enzymatic activity (%). (**B**) Cleavage result of 10 nM ds_dF:dC or ds_rF:dC radioactive substrates using 12.5 ng of whole HeLa cell extracts untreated (*lanes 1, 3*) and treated (*lanes 2, 4*) with 0.20 nM of Compound #3, a specific APE1-endonuclease inhibitor, at 37°C for 10 min. The black arrows on the left of the gel image indicate the size of uncut and cut substrates following denaturation. The cleavage percentage of this experiment is displayed below the image as enzymatic activity (%). (**C**) Histograms showing data from four independent experimental replicas shown in panel (B) with ranges as bars. *P* values of <0.05 are marked by asterisk. WCE, whole cell extracts.

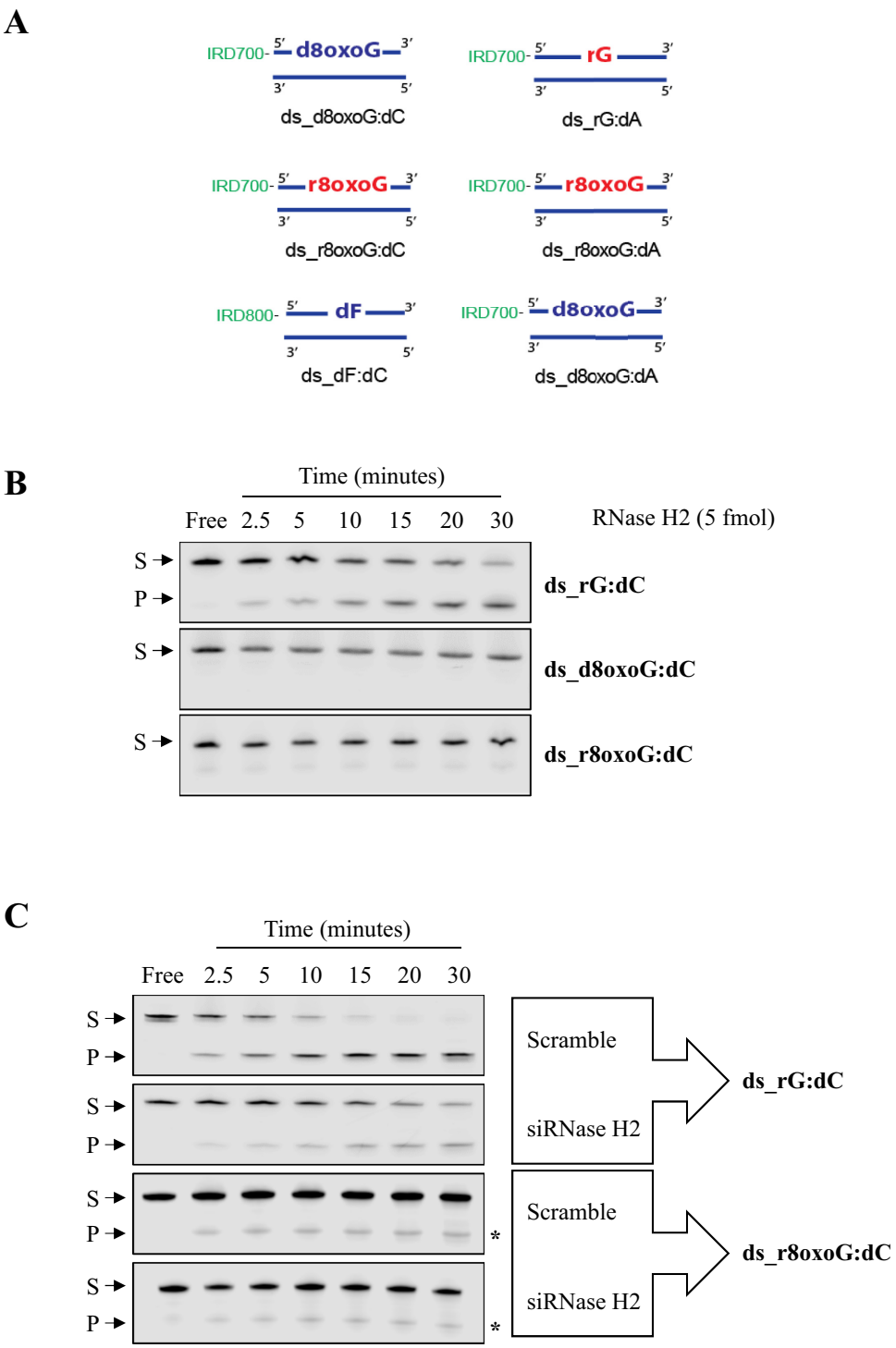

Figure 7. Human RNase H2 is not able to process an r8oxoG site embedded in a duplex DNA substrate. (**A**) Scheme of ds_DNA 25-mer substrates (single strand (ss) oligonucleotide annealed to ss_dC containing- or ss_dA containing-complementary oligonucleotide) containing a d8oxoG, r8oxoG and dF site in the 13th position. The 'IRD700' and 'IRD800' in green indicates IRDye 800 phosphoramidite and IRDye700 phosphoramidite dye tagged at the 5′ end. (**B**) Representative denaturing polyacrylamide gel of oligonucleotides (25 nM) incision by human recombinant RNase H2 (5 fmol). Reaction was performed in RNase H2-buffer (20 mM Tris–HCl, 25 mM KCl, 0.1% BSA, 0.01% Tween20, 4 mM $MgCl_2$, pH 7.4) at 37°C. ds_rG:dC and ds_d8oxoG:dC oligonucleotides were used as positive and negative controls, respectively. Time points are shown on the top of the figure. S indicates the substrate position, while P indicates the product position. (**C**) Representative denaturing polyacrylamide gel of oligonucleotides (0.25 μM) incision by nuclear HeLa cell extracts (NCE). In order to discriminate the activity of RNase H2, 500 ng of NCE in which RNase H2 expression was previously knocked down through specific siRNA (indicated as siRNase H2) were tested in comparison to control cells (Scramble) at different time points (minutes), shown on top of the figure. The endoribonuclease activity detected for r8oxoG oligonucleotide was indicated with an asterisk on the right side of each panel. S indicates the substrate position while P indicates the product position.

OGG1 has neither lyase nor glycosylase activities on oxidized rG substrate

We then tested whether enzymes of the BER pathway may be involved in processing the r8oxoG substrate. To this purpose, we used recombinant purified human OGG1 and APE1 proteins (Supplementary Figure S4A and S5C). OGG1 protein belongs to the bi-functional glycosylases family having both lyase and glycosylase activities on oxidized dG (57). We examined the processing activity of OGG1 on r8oxoG substrate in comparison to the d8oxoG-containing oligonucleotide, as a positive control. First, we tested the ability of OGG1 to recognize an r8oxoG site through electrophoretic mobility shift assay (EMSA). As shown in Figure 8A, increasing amount of recombinant OGG1 formed a stable retarded complex with the r8oxoG oligonucleotide in a dose-dependent manner. As confirmed in the data shown in Supplementary Figure S5E, OGG1 binding was specific for the modified r8oxoG- containing oligonucleotide (*lanes 2 and 3*). Indeed, the same retarded band was observed when the recombinant OGG1 was incubated with the positive control ds_d8oxoG:dC (*lanes 11 and 12*) but not with the negative controls: ds_rG:dC (*lanes 5 and 6*) and ds_dG:dC (*lanes 8 and 9*).

Furthermore, we tested the lyase activity of OGG1 on different substrates. Figure 8B shows that when we incubated increasing amounts of recombinant protein for 30 min at 37°C with different substrates, OGG1 was able to process only the canonical substrate ds_d8oxoG:dC in a dose response manner (Supplementary Figure S5D), whereas no lyase activity was apparent for any of the other substrates used, including the ds_r8oxoG:dC and the ds_r8oxoG:dA.

Since OGG1 is the major glycosylase enzyme in the BER pathway, coordinating with the downstream endonuclease APE1, which is able to recognize and process the abasic site generated by the glycosylase activity of OGG1 (28,58,59), we measured its glycosylase activity on the same substrates using recombinant purified APE1 (Figure 8C). In this case, we co-incubated a fixed amount of recombinant OGG1 with increasing amounts of APE1 for 30 min. While OGG1 displayed a robust glycosylase activity on the canonical ds_d8oxoG:dC substrate, particularly in the presence of the APE1 protein, we detected only a weak activity on ds_r8oxoG:dC oligonucleotide (indicated by a single asterisk) (Figure 8D). Moreover, the presence of an additional higher mobility band, increasing as a function of APE1 concentration (indicated with a double asterisk) was observed only in the case of the ds_r8oxoG:dC substrate. We conclude that OGG1 has neither lyase nor glycosylase activity on the r8oxoG substrate, and that APE1 can weakly process this substrate alone. About APE1 activity, a detailed description is explained in the next paragraph.

APE1 has a weak endo-/exo-nuclease activities on the r8oxoG-containing substrate depending on Mg^{2+} concentration and on the presence of its N-terminal domain

Based on the above presented data, we then checked whether APE1 '*per se*' had any endoribonuclease activity on ds_r8oxoG:dC substrate (Figures 9 and 10). Compared to the ds_dF:dC substrate, APE1 displayed a modest, though significant, processing activity on both ds_r8oxoG:dC and ds_r8oxoG:dA oligonucleotides, while no activity was observed in the case of the dG- and the d8oxoG-containing substrates (Figure 9, panels A and B), as expected. As observed above, the appearance of an additional faster migrating cleavage product (indicated by a double asterisk corresponding to a 11-nt product in Figure 8D) was visible in the case of the ds_r8oxoG:dC substrate, which might be associated with a recently identified 3′-exonuclease activity by the protein (42). We checked the occurrence of the cleavage at the expected ribonucleotide sites, by oligonucleotide sequences of increasing length, ranging from 10 to 16 nucleotides, as molecular markers (Supplementary Figure S6A) and through alkaline hydrolysis experiments (Supplementary Figure S6B). As it is visible (Supplementary Figure S6A), cleavage products of the ds_r8oxoG:dC oligonucleotide were of the expected size and comprised between 11- and 12-nucleotides and are thus compatible with endonucleolytic cleavage occurring only at the 5′ side of the lesion (fragment 12-nt long) and with a 3′-exonuclease activity giving rise to the fragment of 11-nt long. In order to exclude that the observed cleavage product was due to the processing of a residual non-annealed oligonucleotide possibly present after the annealing reaction, we incubated APE1 protein with single stranded oligonucleotide (ss_r8oxoG) and compared the cleavage product with the annealed oligonucleotide (ds_r8oxoG:dC). Comparing the result with both ss_dF and ds_dF:dC oligonucleotides, a product was detectable only using the double stranded oligonucleotides as substrates. No bands were observed using the ss_r8oxoG oligonucleotide (Supplementary Figure S6C) demonstrating the requirement for secondary structured oligonucleotide sequences for efficient enzymatic activities by APE1. In contrast, using the oligonucleotide containing the mismatched ds_r8oxoG:dA, most of the fragments produced after incision by the AP endonucleolytic activity (indicated with a single asterisk) were not further degraded by the exonucleolytic activity (Figure 9A). Therefore, these data demonstrate that the APE1 enzymatic activity on the r8oxoG substrate requires a dsDNA molecule and exonuclease activity is dependent on the paired nucleotide, possibly as a consequence of a different stereochemical geometry between the 8oxoG:A and the 8oxoG:C.

It has been previously demonstrated that the exonuclease activity of APE1 strictly depends on salt concentrations (60). We therefore tested whether the 3′-exonuclease activity observed on the ds_r8oxodG:dC shared some common features (in terms of dependence on the ionic strength conditions) with the 3′-exonuclease activity on mispaired DNA, as previously described (60). Firstly, we determined the optimal $MgCl_2$ (Figure 10A) and KCl (Figure 10B) concentrations required for the 3′-exonuclease activity. Indeed, the 3′-exonuclease activity was present up to a concentration of 2 mM $MgCl_2$. An inhibitory effect was apparent at $MgCl_2$ concentrations above 4 mM. At the same time, the 3′-exonuclease activity was poorly affected at KCl concentration equal to 100 mM. These results are in line with previous data on 3′-mispaired DNA (60) and suggest that the observed 3′-exonuclease activity strongly depends on the electrostatic interaction of APE1 with the substrate during the cleavage reaction and with the role of Mg^{2+} ions.

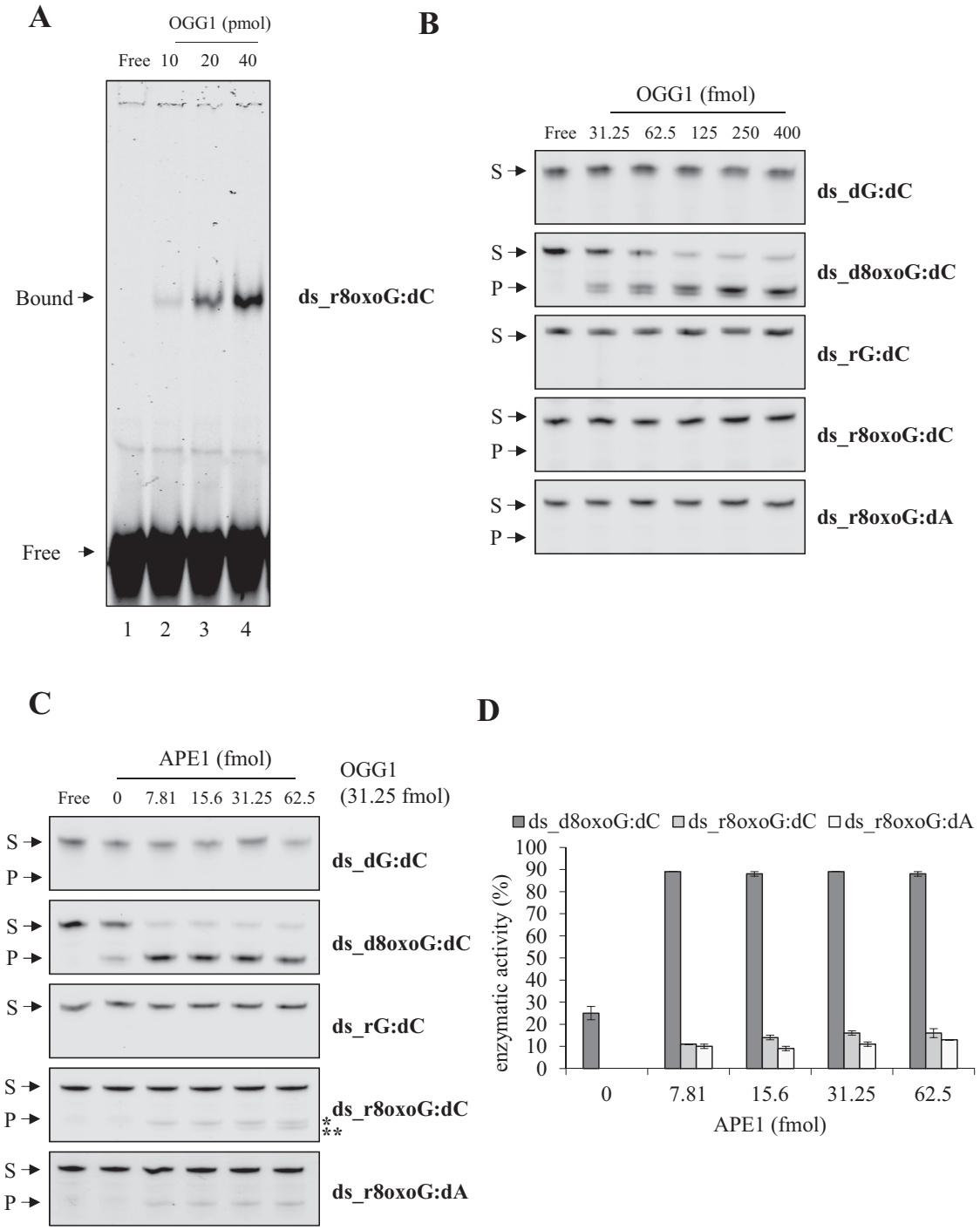

Figure 8. Human OGG1 has neither lyase nor glycosylase activities on r8oxoG-containing oligonucleotide. (**A**) Representative native EMSA polyacrylamide gel of OGG1 binding on ds_r8oxoG:dC oligonucleotide (25 nM) is shown. The 'Bound' arrow indicates the retarded complex between OGG1 and the probe whereas the 'Free' arrow the unbound substrate. Amounts of OGG1 protein, expressed in *pico* moles, are shown on the top of the figure. Reactions were performed as explained in 'Materials and Methods' section**.** (**B**) Representative denaturing polyacrylamide gel of lyase activity of human OGG1 on different duplex DNA oligonucleotides (25 nM). Doses of OGG1 protein expressed in *femto* moles are shown on the top of the figure. Reactions were performed in OGG1-buffer (20 mM Tris–HCl, 100 mM KCl, 0.1% BSA, 0.01% Tween20, pH 7.4) at 37°C for 30 min. S indicates the substrate position, while P indicates the product position. (**C**) Representative denaturing polyacrylamide gel of incision by different doses of APE1 co-incubated with a fixed amount of OGG1 (3.125 nM) on different duplex DNA oligonucleotides (25 nM) in order to investigate glycosylase activity of OGG1. Different doses of APE1 protein, expressed in *femto* moles, are shown on top of the figure. Reactions were performed in a buffer containing 20 mM Tris–HCl, 100 mM KCl, 0.1% BSA, 0.01% Tween20, pH 7.4 at 37°C for 30 min. S indicates the substrate position while P indicates the product position. Moreover, at the right of the panel, a longer product of about 12 nucleotides is indicated by an asterisk whereas a smaller one of 11 nucleotides is indicated by a double asterisk. (**D**) Histograms represent the dose response of OGG1 glycosylase activity on ds_d8oxoG:dC and paired and mismatched ds_r8oxoG oligonucleotides. ds_d8oxoG oligonucleotide was used as a positive control whereas ds_dG:dC and ds_rG:dC oligonucleotides were used as negative controls. The activity is reported as percentage of substrate converted to product. Data are expressed as mean ± SD of three independent technical replicas.

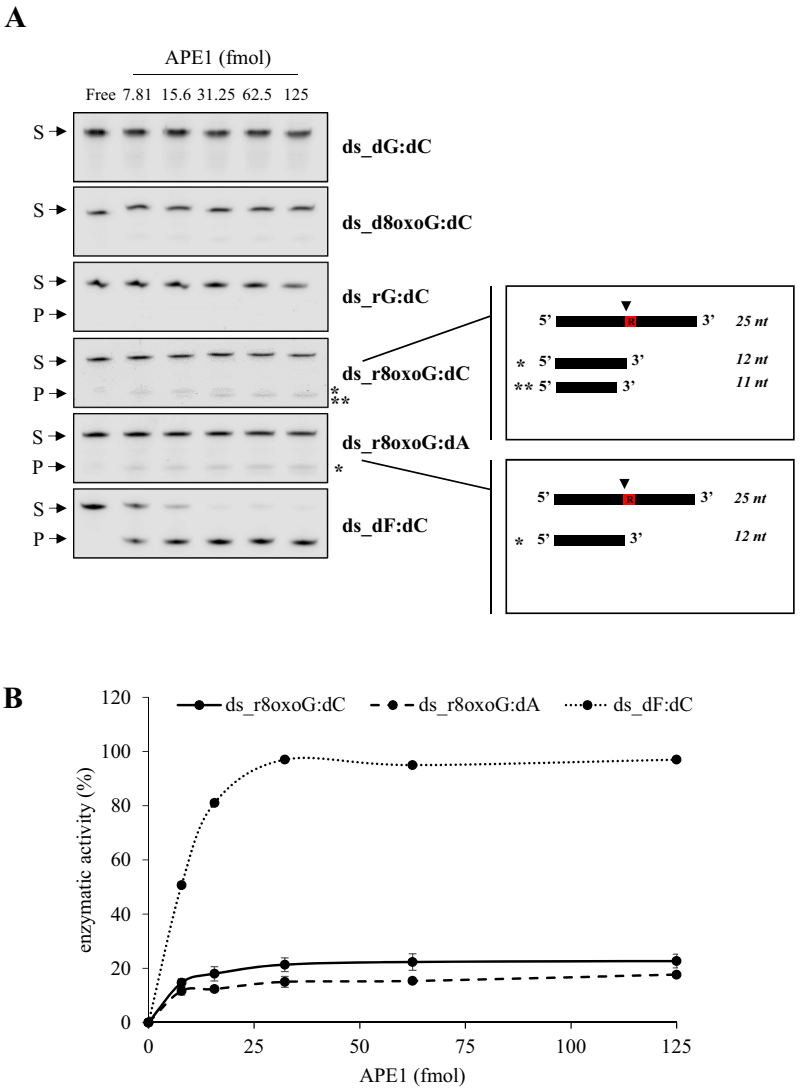

Figure 9. Human APE1 shows a weak endo- and a 3′-exonuclease activities on r8oxoG substrate. (**A**) Representative denaturing polyacrylamide gel of APE1 incision on different duplex DNA oligonucleotides (25 nM), in which ds_dF:dC oligonucleotide was used as a positive control, whereas ds_dG:dC and ds_rG:dC oligonucleotides were used as negative controls. The doses of APE1 protein used, expressed in *femto* moles, are shown on the top of the figure. On the right side, a schematic representation of the cleavage products, showing the position of the ribonucleotide (red box with R) embedded in the DNA oligonucleotide and the APE1 cleavage on it, producing a longer product of about 12 nucleotides (*) and a smaller one of 11 nucleotides (**). Reactions were performed in APE1-buffer containing 20 mM Tris–HCl, 100 mM KCl, 0.1% BSA, 0.01% Tween20, pH 7.4 for 30 min at 37°C. S indicates the substrate position while P indicates the product position. (**B**) Relative graph indicates a dose–response APE1 activity on paired and mismatched ds_r8oxoG:dC oligonucleotide in comparison to ds_dF:dC positive control. Data are expressed as mean ± SD of three independent technical replicas.

After choosing the optimal salts conditions, in which both endo- and exo- activities of APE1 (100 mM KCl and 1 mM $MgCl_2$) are present, we then evaluated whether the enzymatic activity of APE1 on ds_r8oxoG:dC was dependent on the same catalytic site responsible for the endonuclease activity observed on abasic dsDNA and abasic rNMP. To this aim, the enzymatic activity of the E96A mutant was compared to that of the WT protein (Supplementary Figure S6D). These data demonstrate that the APE1 E96A mutant has a reduced endoribonuclease activity showing no 3′-exonuclease activity over the ds_r8oxoG:dC substrate. Due to the effect of salt concentration on this latter activity, we also tested the enzymatic activity of the APE1 NΔ33 deletion mutant (Supplementary Figure S6D). Interestingly, while this protein retained the endoribonuclease activity of the WT protein, its 3′-exonuclease activity was abolished. Moreover, treatment with APE1 inhibitor Compound #3 confirmed that the catalytic site responsible for the endonuclease activity is also responsible for the endoribonuclease activity over the r8oxoG substrate (Supplementary Figure S6E). These results show that APE1 has a weak, though significant, endoribonuclease activity on r8oxoG substrates with an additional specific 3′-exonuclease activity dependent on: (i) the kind of pair: i.e. ds_r8oxoG:dC or ds_r8oxoG:dA; (ii) salt concentrations (i.e. Mg^{2+}); (iii) the presence of the 33 N-terminal domain.

Overall, our data demonstrate that BER enzymes but not RER are involved in the processing of non-canonical rN-

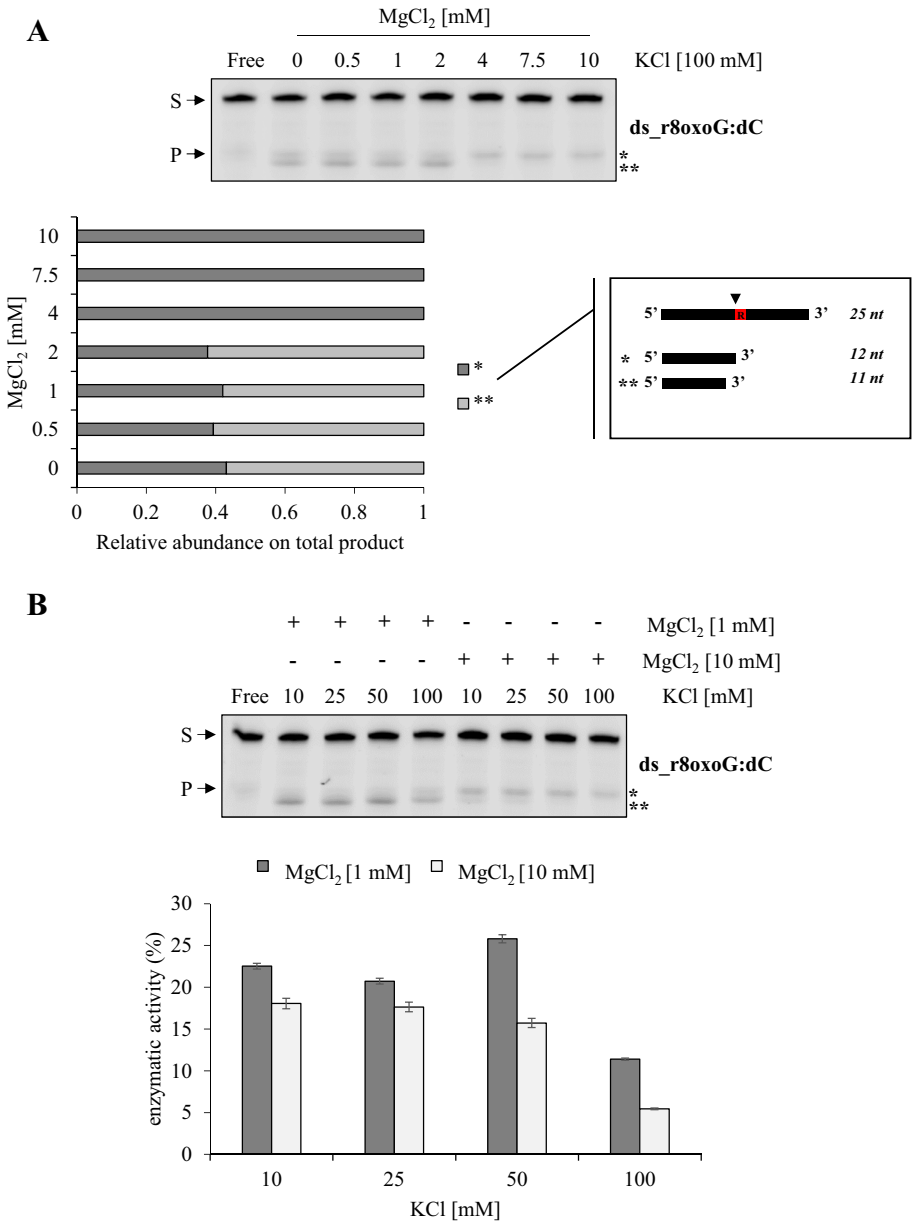

Figure 10. Human APE1 activities on r8oxoG substrate depend on mono- and di-valent cations. (**A**) Representative denaturing polyacrylamide gel of APE1 (5 nM) incision on ds_r8oxoG:dC oligonucleotide under different $MgCl_2$ concentrations that is expressed in mM (*top*) performing a reaction long 30 minutes in APE1 buffer. S indicates the substrate position while P indicates the product position. Moreover, at the right of the panel, a longer product of about 12 nucleotides is indicated by an asterisk whereas a smaller one of 11 nucleotides is indicated by a double asterisk Also shown on the right is a schematic representation of the cleavage products, showing the position of the ribonucleotide (red box with R) embedded in the DNA oligonucleotide and the APE1 cleavage on it, producing a longer product of about 12 nucleotides (*) and a smaller one of 11 nucleotides (**). Relative graph shows the ratio between two products obtained as a function of $MgCl_2$ concentration (*bottom*). (**B**) Representative denaturing polyacrylamide gel of APE1 (5 nM) incision on ds_r8oxoG:dC oligonucleotide under different KCl concentrations in combination with two different $MgCl_2$ concentrations, 1 mM and 10 mM (*top*) performing a reaction long 30 min in a buffer containing 20 mM Tris–HCl, 0.1% BSA, 0.01% Tween20, pH 7.4. S indicates the substrate position, while P indicates the product position. Moreover, at the right of the panel, a longer product of about 12 nucleotides is indicated by an asterisk whereas a smaller one of 11 nucleotides is indicated by a double asterisk. Relative graph shows product levels in association with different salts concentrations (*bottom*).

MPs, such as abasic or oxidized, incorporated in DNA. Because the repair pathway catalyzed by APE1 toward the oxidized rG is fundamentally different from that of BER, since no bases are excised, we can conclude that the observed effect could be ascribed to an alternative damage-specific endonuclease initiated repair pathway, previously referred to as either alternative excision repair (AER) or nucleotide incision repair (NIR) (reviewed in (61,62)).

APE1 and RNase H2 do not biochemically and functionally interact in human cells

To support the functional independence between BER and RER, we tested whether APE1 and RNase H2 proteins

functionally interact. We tested whether this hypothesis was confirmed in HeLa cells transfected with siRNAs specific for APE1 and RNase H2 mRNAs to knock down the corresponding endogenous proteins. Whole cell extracts were prepared as explained in Materials and Methods section, and western blotting analysis was used to check the effective protein down regulation (Supplementary Figure S7A). Then, we checked the ability of APE1 and RNase H2 from cell extracts to recognize the ds_r8oxoG:dC substrate. We performed EMSA with cell extracts from control (Scramble) and APE1-kd (siAPE1) or RNase H2-kd (siRNase H2) cells. As demonstrated in Supplementary Figure S7B, incubation of cell extract from control cells displayed a retarded band containing APE1-complex, as also demonstrated by supershift EMSA experiments with anti-APE1 specific antibody (Supplementary Figure S7, panels C and D). The intensity of the retarded complex was decreased upon APE1-kd (siAPE1) (Supplementary Figure S7B, lane 4) and upon the double APE1/RNase H2-kd (siAPE1 + siRNase H2) (*lane 6*) but not upon RNase H2 silencing alone (siRNase H2) (*lane 5*), confirming that APE1 is involved in a protein complex able to recognize r8oxoG damage in which RNase H2 is not present.

DISCUSSION

Increased body of evidence supports the notion that incorporation of rNMPs in DNA is a frequent phenomenon, having profound detrimental effects on genome stability of both prokaryotes and eukaryotes (1,2,63,64). In humans, as well as in yeast and bacteria including Archaea, the main processing pathway responsible for repairing of these lesions is the RER pathway, which involves the RNase H2 enzyme (65,66). RNase H2 importance in higher organisms is testified by its essentiality for embryonic development in mouse (67). Moreover, RNase H2 mutations in humans are causally linked to the onset of AGS, a rare autoimmune inflammatory disease (68,69). It can be hypothesized that among the many millions rNMPs that are introduced in the mammalian genome per cell cycle (3), not only canonical rNMPs are incorporated but also damaged rNMPs (such as abasic and oxidized). Indeed, like deoxyribonucleotides, rNMPs are also susceptible to oxidative insults (5,70), and a significant generation of abasic sites formation has been demonstrated upon RNA oxidation and alkylation (71). While the role of RNase H2-initiated RER mechanism of DNA repair in recognizing and cleaving rNMPs embedded in DNA is well established (3,15), nothing is known regarding the DNA repair pathways involved in the removal of damaged rNMPs.

BER is the main mechanism coping with the repair of non-distorting single-base lesions, such as abasic sites and oxidized bases (27). Interestingly, emerging literature, including ours, pointed to a new function of BER in RNA quality control surveillance and RNA-decay with the functions of SMUG1, PARP1 and APE1 in RNA processing (38,72). At present, however, there is no evidence that BER may cope with the removal of rNMPs from DNA. Identifying whether BER may target unmodified and/or modified rNMPs in DNA is important to better understanding the mechanism of genotoxicity of oxidative stress and the impact of BER defects in human disease, cancer mechanisms, and for the development of new anticancer strategies.

In this work, we demonstrate that an rAP site embedded in DNA is targeted by APE1 of BER rather than RER in eukaryotic systems (Figure 11A). We have found that eukaryotic RNase H2 enzymes from yeast, mouse and human, and from human cell extracts are unable to process rAP sites in DNA, whereas recombinant human APE1 is able to efficiently cleave this type of damage (Figures 2 and 3). APE1 processes the rAP site as efficiently as the canonical deoxy-abasic site as measured by kinetic data (Table 1). Data using catalytic inactive APE1 mutants (E96A) clearly demonstrate that the endonuclease active site of APE1 is required to perform the endoribonuclease activity on a ribose abasic site in dsDNA. Differently, the cleavage activity of the 33N-terminal truncated mutant, which does not impact the catalytic function of the enzyme but is involved in the release of the product upon cleavage (48), is comparable to that of wild-type APE1. This last result demonstrates that the unstructured N-domain is dispensable for the enzymatic reaction on the abasic ribonucleotide site. Moreover, using HeLa nuclear cell extracts that were siRNA-depleted of APE1 or RNAse H2 proteins, we showed that the processing activity of the rAP site in DNA depends only on the presence of APE1 and not on RNase H2. These results highlight a new role of APE1 in repairing rAP sites embedded in DNA, demonstrating that the catalytic site of APE1 and the mechanism of product release is similar to that of the canonical deoxy-substrate.

rAP sites embedded in DNA may be generated by spontaneous hydrolysis or by the action of an unknown glycosylase on oxidized rNMPs, such as r8oxoG. Furthermore, a potentially significant, yet poorly characterized, source of rNMPs incorporated in DNA is the oxidative stress. rNMPs were shown to form during oxidative DNA damage both *in vitro* and *in vivo* (5). Therefore, it is also possible that abasic and oxidized DNA is converted into RNA. It was estimated that spontaneous depurination occurs 1,000 times slower in RNA than DNA (73). For example the rate of depurination in DNA under physiological conditions is estimated to be 1 out of 100 000 purines every cell cycle. This rate gives 10 000 abasic sites per day in human cells (74). Considering the remarkable abundance of rNMPs in DNA, which could be as many as 600 000 rNMPs in budding yeast genomic DNA, and therefore a factor of 250 higher in mammalian genomic DNA (150 000 000) (3), i.e. >300 millions in the human diploid DNA per cell cycle, it is not unrealistic to anticipate that cells may contain a non-negligible number of rAP sites in DNA, or oxidized rNMPs. Interestingly, abasic RNA results significantly more stable than abasic DNA, suggesting that specific enzymatic mechanisms should exist *in vivo* to cope with this harmful lesion (75). In addition, in conditions of oxidative DNA damage, such as in cancer cells, the likelihood of such base modifications can increase. Moreover, recent studies already suggested that r8-oxoGTP is formed *in vivo* under oxidative stress conditions and may be incorporated during replication into DNA by *S. pombe*, *M. smegmatis* and human (34–36). Moreover, the introduction of r8oxoG in DNA can be catalyzed by human DNA Polβ (36). However, the level and function of Polβ in cells are highly regulated by complex signaling mecha-

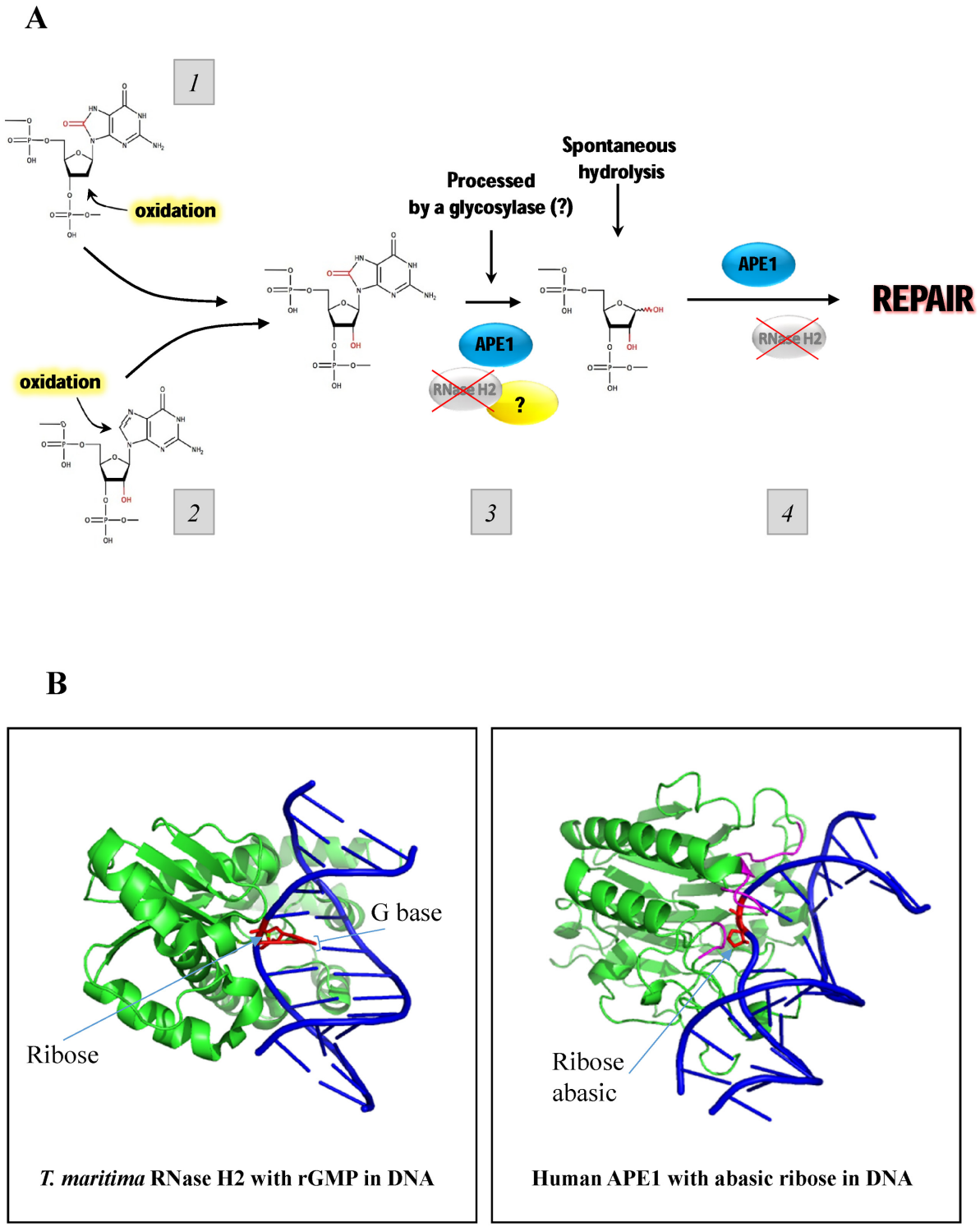

Figure 11. Model for repair of oxidized rNMPs and rAP sites embedded in DNA by APE1. (**A**) 8oxo-ribonucleotides could be generated in the cellular nucleotide pool or even when they are already incorporated in DNA as a result of an oxidation of the sugar (1) and/or the base (2). After the evidence that human RNase H2 is not able to process an oxidized rNMP embedded in DNA, we found that APE1 shows a weak but significant activity on it (3). Similarly, RNase H2 does not process an rAP embedded in DNA, which could be generated spontaneously or by the r8oxoG processing, and again APE1 possesses a strong activity on this type of damage (4). Because APE1 activity on 8oxo-ribonucleotides in DNA is low, we hypothesize that other proteins (some glycosylases?) may participate in their repair. (**B**) Structural models with the active site of RNase H2 and APE1 with an rNMP or an rAP. *T. maritima* (left) and human APE1 (right) is in a complex with DNA having a single rNMP or single abasic residue, respectively. DNA is indicated in blue, while the single rNMP and the abasic residues are shown in red as sticks. The arrows points towards ribose or G base or abasic sites in the panels. Proteins are shown in green except for three of the several regions on APE1 that engulf the abasic sugar which are in magenta. PDB for RNase H2 is 303-F; for APE1 as 1DEW (92).

nism and interactome networks (76). Therefore, the probability of r8oxoG incorporation into genomic DNA by Polβ is still a question under debate, which needs further experimental proof. Spontaneous formation of rAP sites being a rare event, it is a key question to find activities producing rAPs following processing of oxidized rNMPs in DNA. In addition, a possible RER and BER involvement in removal of r8oxoG from DNA has been proposed in other reports (36,77). Work in our laboratory is ongoing along these lines to address these fundamental issues. Considering these observations, we focused our attention on which BER protein, if any, may be involved in recognition and cleavage of oxidized rNMPs (r8oxoG) embedded in DNA. First, we tested the RNase H2 activity on r8oxoG substrate (Figure 7). Similarly to results with the abasic rNMP in DNA our data clearly demonstrate that RER is not involved in processing of oxidized rNMPs embedded in DNA. Based on these findings, we explored a potential role of the BER pathway. First, we showed that the human OGG1, the main glycosylase enzyme able to recognize and repair oxidized dG through its lyase and glycosylase activities, has neither a lyase nor a glycosylase activity on an oxidized rG site embedded in a DNA substrate, despite its ability to efficiently bind the oxidized substrate (Figure 8), in agreement with recent findings (77). Interestingly, we discovered that APE1 has a weak endoribonuclease activity on r8oxoG site embedded in a DNA substrate, and shows a 3′-exonuclease activity (Figures 9 and 10), similarly to the 3′-exonuclease activity on DNA demonstrated previously (52,54). In line with previous results, the 3′-exonuclease activity of APE1 is strictly dependent on Mg^{2+} concentration and on the presence of the first 33 aminoacids. The importance of the N-terminal domain is to be attributed to different reasons: (i) it bears the majority of the positive charges of APE1; (ii) is the target of the main post-translational modifications of the protein (i.e. acetylation, ubiquitination, proteolysis); (iii) is involved in modulating the interaction with different protein partners and finally (iv) may modulate the catalytic rate, probably acting on the k_{off} of the catalytic reaction due to increased speed of product release (37,48,78). These unexpected results, which suggest that APE1 3′-exonuclease activity strongly depends on the electrostatic interaction of APE1, involving its unstructured N-terminal domain, with the substrate (52), may be explained on the basis of the previously characterized ability of APE1 to process some particular structured RNA species in a specific manner (37).The activity of APE1 on r8oxoG embedded in DNA does not hide the possibility that a similar activity could be exerted on RNA molecules too. This finding could represent the first demonstration of an enzyme able to recognize and process oxidized RNA (78). To date, RNA oxidation has been shown to exert detrimental physiological effects and to be a common feature in different human pathologies ranging from ageing to neurodegenerative and cancer diseases (79). For instance, oxidized RNA (80) or RNA containing abasic sites (75) show inhibitory effects on reverse transcriptase activity, whereas oxidized mRNA (81,82) or mRNA with abasic sites (83) exhibit compromised translation activity as well as translation fidelity (84). The weak endo- and 3′-exonuclease activities on r8oxoG- containing substrate and their dependence on Mg^{2+}-concentrations and on the presence of the first N-terminal domain residues of APE1 are fully in agreement with the previously described nucleotide incision repair (NIR) function by APE1 on several oxidized substrates, such as: 5,6-dihydro-2′-deoxyuridine, 5,6-dihydrothymidine, 5-hydroxy-2'-deoxyuridine, 5-hydroxycytosine (43–45). Notably, the limited activity obtained in the experimental conditions we used (also after changing the pH conditions, data not shown) are in agreement with previous reports on the NIR function by APE1 on some particular substrates such as the αdG:dG and the 5OH-dC:dG (44). In addition, the biochemical characterization through MALDI-MS and HPLC analyses we performed (Supplementary Figure S5 panels A and B) may be suggestive for the existence of an equilibrium between different conformational species of r8oxoG dsDNA, excluding any possible bias due to contaminant present in the oligonucleotide used for the assays. Therefore, these findings underscore the importance of identifying the enzyme(s) responsible for the recognition and efficient processing of the r8oxoG substrate, in order to further extend our studies and our understanding of this hot scientific topic.

We observed that OGG1 is unable to process the r8oxoG substrate, while being perfectly able to specifically bind it, similar to what recently published by Sassa *et al*. (77). At present, it is possible to speculate that though the base-flipping occurs, the enzymes is unable to hydrolyze the N-glycosidic bond and has no lyase activity maybe as a consequence of the steric hindrance with the 2′OH of the ribose which renders the C1′ unavailable for the nucleophilic attack by the catalytic site. Differently from our results, Sassa *et al*. found no enzymatic activity by APE1. This discrepancy with our results may be due to the different experimental conditions for the enzymatic assays, i.e. higher Mg^{2+} concentrations and the use of a small amount of EDTA, both aspects already demonstrated to strongly affect the APE1 enzymatic activity on the r8oxoG substrate. A comparative experiment we performed (Supplementary Figure S8) was indeed supportive of this hypothesis, reinforcing the importance of the experimental conditions when studying the non-canonical functions of APE1 protein. Interestingly, Sassa *et al.* showed that the commercially available prokaryotic RNase HII preserves the ability to remove an oxidized rNMP in a DNA duplex. Contrary to these results, our findings show that eukaryotic RNase H2 is completely inactive on a substrate containing an oxidized rNMP. These data suggest that the ability to process r8oxoG in DNA has been lost during evolution and deserves further studies.

To explain why APE1 recognized the abasic rNMP in DNA and RNase H2 did not, we compared the model structures of DNA with an rNMP or an rAP site in the RNase H2 and APE1 active site, respectively (Figure 11B). RNase H2 recognizes the RNA-DNA junction with the substrate participating in catalysis. Prior to incision by RNase H2, the rNMP base is hydrogen bonded to the complementary DNA strand base (85). If the rNMP is abasic, there is no hydrogen bonding to stabilize the complex required for RNase H2. Rather, an orphan base on the complementary DNA strand is present. We hypothesized that the lack of the hydrogen bonding between the abasic rNMP and the opposite deoxyribonucleotide interferes with the capacity of RNase

H2 to recognize an abasic rNMP and cleave it. Thus, the role of recognizing and cleaving abasic rNMPs is not specific of RNase H2. Differently from RNase H2, APE1 specifically recognizes and cleaves an abasic distortion in DNA, and basically engulfs the sugar-phosphate further distorting the DNA (86), as seen in Figure 11B. Here, we predicted that the ribose extra OH would have only minor influence on the structure. Therefore, this could explain why the abasic rNMP, like an abasic deoxyribonucleotide in DNA, was efficiently cleaved by APE1.

Experiments are underway in order to address if other glycosylases may process oxidized rNMPs in order to generate rAP sites, which are then efficiently processed by APE1. We previously demonstrated that APE1-defective cells have increased oxidized rRNA content upon oxidative stress (37). This result has now a molecular explanation in the observed endoribonuclease activity of APE1 over r8oxoG containing oligonucleotides and will deserve further attention in our future studies. Regarding the formation of abasic ribonucleotides in DNA, this is still a matter of debate. The existence of specific N-ribohydrolases, including the toxin ricin, has been already documented (87) to be able to generate abasic rNMPs in RNA molecules, besides spontaneous generation (71). A role for the YB-1 protein in recognizing oxidized ribonucleotides sites in RNA has also been hypothesized (88), but no specific enzymatic mechanisms able to remove the oxidized base has been described, yet. The accumulation of the r8oxoG substrates, which occurs on RNA upon silencing of APE1 expression, may thus be explained under the assumption that enzymatic removal of oxidized rNMPs may represent the limiting step in the process. Besides its direct activity on r8oxoG, APE1 could be stimulated by a glycosylase activity allowing a faster turnover as demonstrated for DNA substrates (89). Work is in progress along these lines to better inspect this mechanism and the putative glycosylase enzymes involved. Moreover, since APE1 is overexpressed in different types of cancer, such as ovarian, gastro-esophageal, pancreatico-biliary, lung and breast cancers (90,91), it would be interesting to determine whether any correlation exists between its expression level and presence of modified rNMPs in cancers.

SUPPLEMENTARY DATA

Supplementary Data are available at NAR Online.

ACKNOWLEDGEMENTS

The authors thank the Tell and Storici laboratories for constructive feedback. They are also grateful to the funding sources listed below for supporting this work. The authors thank Bret Freudenthal for his fruitful comments during manuscript preparation.

FUNDING

National Institute of Health (NIH) [R01ES026243-01 to F.S.]; Howard Hughes Medical Institute Faculty Scholar [55108574 to F.S.]; Italian Association for Cancer Research (AIRC) [IG2013-14038 to G.T.]; Intramural Research Program of National Institute of Child Health and Human Development [to R.J.C.]. Funding for open access charge: NIH [1R01ES026243-01 to F.S.]; Research funds from the University of Udine (to G.T.).
Conflict of interest statement. None declared.

REFERENCES

1. Williams,J.S. and Kunkel,T.A. (2014) Ribonucleotides in DNA: origins, repair and consequences. *DNA Repair*, **19**, 27–37.
2. Koh,K.D., Balachander,S., Hesselberth,J.R. and Storici,F. (2015) Ribose-seq: global mapping of ribonucleotides embedded in genomic DNA. *Nat. Methods*, doi:10.1038/nmeth.3259.
3. Williams,J.S., Lujan,S.A. and Kunkel,T.A. (2016) Processing ribonucleotides incorporated during eukaryotic DNA replication. *Nat. Rev. Mol. Cell Biol.*, **17**, 350–363.
4. Clausen,A.R., Zhang,S., Burgers,P.M., Lee,M.Y. and Kunkel,T.A. (2013) Ribonucleotide incorporation, proofreading and bypass by human DNA polymerase δ. *DNA Repair*, **12**, 121–127.
5. Randerath,K., Reddy,R., Danna,T.F., Watson,W.P., Crane,A.E. and Randerath,E. (1992) Formation of ribonucleotides in DNA modified by oxidative damage in vitro and in vivo. Characterization by 32P-postlabeling. *Mutat. Res.*, **275**, 355–366.
6. Nick McElhinny,S.A., Watts,B.E., Kumar,D., Watt,D.L., Lundstrom,E.-B., Burgers,P.M.J., Johansson,E., Chabes,A. and Kunkel,T.A. (2010) Abundant ribonucleotide incorporation into DNA by yeast replicative polymerases. *Proc. Natl. Acad. Sci. U.S.A.*, **107**, 4949–4954.
7. Crespan,E., Furrer,A., Rösinger,M., Bertoletti,F., Mentegari,E., Chiapparini,G., Imhof,R., Ziegler,N., Sturla,S.J., Hübscher,U. *et al.* (2016) Impact of ribonucleotide incorporation by DNA polymerases β and λ on oxidative base excision repair. *Nat. Commun.*, **7**, 10805.
8. Traut,T.W. (1994) Physiological concentrations of purines and pyrimidines. *Mol. Cell. Biochem.*, **140**, 1–22.
9. Chiu,H.-C., Koh,K.D., Evich,M., Lesiak,A.L., Germann,M.W., Bongiorno,A., Riedo,E. and Storici,F. (2014) RNA intrusions change DNA elastic properties and structure. *Nanoscale*, **6**, 10009.
10. Koh,K.D., Chiu,H.-C., Riedo,E. and Storici,F. (2015) Measuring the elasticity of ribonucleotide(s)-containing DNA molecules using AFM. *Methods Mol. Biol. Clifton NJ*, **1297**, 43–57.
11. Evich,M., Spring-Connell,A.M., Storici,F. and Germann,M.W. (2016) Structural Impact of Single Ribonucleotide Residues in DNA. *ChemBioChem*, **17**, 1968–1977.
12. Caldecott,K.W. (2014) Molecular biology. Ribose—an internal threat to DNA. *Science*, **343**, 260–261.
13. Storici,F., Bebenek,K., Kunkel,T.A., Gordenin,D.A. and Resnick,M.A. (2007) RNA-templated DNA repair. *Nature*, **447**, 338–341.
14. Shen,Y., Nandi,P., Taylor,M.B., Stuckey,S., Bhadsavle,H.P., Weiss,B. and Storici,F. (2011) RNA-driven genetic changes in bacteria and in human cells. *Mutat. Res. Mol. Mech. Mutagen.*, **717**, 91–98.
15. Cerritelli,S.M. and Crouch,R.J. (2009) Ribonuclease H: the enzymes in eukaryotes: ribonucleases H of eukaryotes. *FEBS J.*, **276**, 1494–1505.
16. Crow,Y.J. and Manel,N. (2015) Aicardi–Goutières syndrome and the type I interferonopathies. *Nat. Rev. Immunol.*, **15**, 429–440.
17. Crow,Y.J., Leitch,A., Hayward,B.E., Garner,A., Parmar,R., Griffith,E., Ali,M., Semple,C., Aicardi,J., Babul-Hirji,R. *et al.* (2006) Mutations in genes encoding ribonuclease H2 subunits cause Aicardi-Goutières syndrome and mimic congenital viral brain infection. *Nat. Genet.*, **38**, 910–916.
18. Rice,G., Patrick,T., Parmar,R., Taylor,C.F., Aeby,A., Aicardi,J., Artuch,R., Montalto,S.A., Bacino,C.A., Barroso,B. *et al.* (2007) Clinical and molecular phenotype of Aicardi-Goutières Syndrome. *Am. J. Hum. Genet.*, **81**, 713–725.
19. Brzostek-Racine,S., Gordon,C., Van Scoy,S. and Reich,N.C. (2011) The DNA damage response induces IFN. *J. Immunol.*, **187**, 5336–5345.
20. Reijns,M.A.M., Rabe,B., Rigby,R.E., Mill,P., Astell,K.R., Lettice,L.A., Boyle,S., Leitch,A., Keighren,M., Kilanowski,F. *et al.* (2012) Enzymatic removal of ribonucleotides from DNA is essential for mammalian genome integrity and development. *Cell*, **149**, 1008–1022.
21. Williams,J.S., Smith,D.J., Marjavaara,L., Lujan,S.A., Chabes,A. and Kunkel,T.A. (2013) Topoisomerase 1-mediated removal of

ribonucleotides from Nascent leading-strand DNA. *Mol. Cell*, **49**, 1010–1015.
22. Potenski,C.J., Niu,H., Sung,P. and Klein,H.L. (2014) Avoidance of ribonucleotide-induced mutations by RNase H2 and Srs2-Exo1 mechanisms. *Nature*, **511**, 251–254.
23. Kim,N., Huang,S., Williams,J.S., Li,Y.C., Clark,A.B., Cho,J.-E., Kunkel,T.A., Pommier,Y. and Jinks-Robertson,S. (2011) Mutagenic processing of ribonucleotides in DNA by yeast topoisomerase I. *Science*, **332**, 1561–1564.
24. Vaisman,A., McDonald,J.P., Huston,D., Kuban,W., Liu,L., Van Houten,B. and Woodgate,R. (2013) Removal of misincorporated ribonucleotides from prokaryotic genomes: an unexpected role for nucleotide excision repair. *PLoS Genet.*, **9**, e1003878.
25. Lindsey-Boltz,L.A., Kemp,M.G., Hu,J. and Sancar,A. (2015) Analysis of ribonucleotide removal from DNA by human nucleotide excision repair. *J. Biol. Chem.*, **290**, 29801–29807.
26. Shen,Y., Koh,K.D., Weiss,B. and Storici,F. (2011) Mispaired rNMPs in DNA are mutagenic and are targets of mismatch repair and RNases H. *Nat. Struct. Mol. Biol.*, **19**, 98–104.
27. Dianov,G.L., Souza-Pinto,N., Nyaga,S.G., Thybo,T., Stevnsner,T. and Bohr,V.A. (2001) Base excision repair in nuclear and mitochondrial DNA. *Prog. Nucleic Acid Res. Mol. Biol.*, **68**, 285–297.
28. Krokan,H.E. and Bjoras,M. (2013) Base excision repair. *Cold Spring Harb. Perspect. Biol.*, **5**, a012583.
29. Sykora,P., Wilson,D.M. and Bohr,V.A. (2012) Repair of persistent strand breaks in the mitochondrial genome. *Mech. Ageing Dev.*, **133**, 169–175.
30. Farrington,S.M., Tenesa,A., Barnetson,R., Wiltshire,A., Prendergast,J., Porteous,M., Campbell,H. and Dunlop,M.G. (2005) Germline susceptibility to colorectal cancer due to base-excision repair gene defects. *Am. J. Hum. Genet.*, **77**, 112–119.
31. Bauer,N.C., Corbett,A.H. and Doetsch,P.W. (2015) The current state of eukaryotic DNA base damage and repair. *Nucleic Acids Res.*, doi:10.1093/nar/gkv1136.
32. Lindahl,T. (1993) Instability and decay of the primary structure of DNA. *Nature*, **362**, 709–715.
33. Kochetkov,N.K. and Budovskii,E.I. (1972) Reactions involving the cleavage or rearrangement of heterocyclic rings of nucleic acid bases and their derivatives. In: Kochetkov,NK and Budovskii,EI (eds). *Organic Chemistry of Nucleic Acids*. Springer, Boston, pp. 381–423.
34. Sastre-Moreno,G., Sanchez,A., Esteban,V. and Blanco,L. (2014) ATP insertion opposite 8-oxo-deoxyguanosine by Pol4 mediates error-free tolerance in Schizosaccharomyces pombe. *Nucleic Acids Res.*, **42**, 9821–9837.
35. Ordonez,H. and Shuman,S. (2014) Mycobacterium smegmatis DinB2 misincorporates deoxyribonucleotides and ribonucleotides during templated synthesis and lesion bypass. *Nucleic Acids Res.*, **42**, 12722–12734.
36. Cilli,P., Minoprio,A., Bossa,C., Bignami,M. and Mazzei,F. (2015) Formation and repair of mismatches containing ribonucleotides and oxidized bases at repeated DNA sequences. *J. Biol. Chem.*, **290**, 26259–26269.
37. Vascotto,C., Fantini,D., Romanello,M., Cesaratto,L., Deganuto,M., Leonardi,A., Radicella,J.P., Kelley,M.R., D'Ambrosio,C., Scaloni,A. *et al.* (2009) APE1/Ref-1 interacts with NPM1 within nucleoli and plays a role in the rRNA quality control process. *Mol. Cell. Biol.*, **29**, 1834–1854.
38. Tell,G., Wilson,D.M. and Lee,C.H. (2010) Intrusion of a DNA repair protein in the RNome world: is this the beginning of a new era? *Mol. Cell. Biol.*, **30**, 366–371.
39. Barnes,T., Kim,W.-C., Mantha,A.K., Kim,S.-E., Izumi,T., Mitra,S. and Lee,C.H. (2009) Identification of apurinic/apyrimidinic endonuclease 1 (APE1) as the endoribonuclease that cleaves c-myc mRNA. *Nucleic Acids Res.*, **37**, 3946–3958.
40. Berquist,B.R., McNeill,D.R. and Wilson,D.M. (2008) Characterization of abasic endonuclease activity of human Ape1 on alternative substrates, as well as effects of ATP and sequence context on AP site incision. *J. Mol. Biol.*, **379**, 17–27.
41. Li,M. and Wilson,D.M. (2014) Human apurinic/apyrimidinic endonuclease 1. *Antioxid. Redox Signal.*, **20**, 678–707.
42. Chohan,M., Mackedenski,S., Li,W.-M. and Lee,C.H. (2015) Human apurinic/apyrimidinic endonuclease 1 (APE1) has 3′ RNA phosphatase and 3′ exoribonuclease activities. *J. Mol. Biol.*, **427**, 298–311.
43. Gros,L. (2004) The major human AP endonuclease (Ape1) is involved in the nucleotide incision repair pathway. *Nucleic Acids Res.*, **32**, 73–81.
44. Daviet,S., Couvé-Privat,S., Gros,L., Shinozuka,K., Ide,H., Saparbaev,M. and Ishchenko,A.A. (2007) Major oxidative products of cytosine are substrates for the nucleotide incision repair pathway. *DNA Repair*, **6**, 8–18.
45. Mazouzi,A., Vigouroux,A., Aikeshev,B., Brooks,P.J., Saparbaev,M.K., Morera,S. and Ishchenko,A.A. (2013) Insight into mechanisms of 3′-5′ exonuclease activity and removal of bulky 8,5′-cyclopurine adducts by apurinic/apyrimidinic endonucleases. *Proc. Natl. Acad. Sci. U.S.A.*, **110**, E3071–E3080.
46. Gasparutto,D., Livache,T., Bazin,H., Duplaa,A.M., Guy,A., Khorlin,A., Molko,D., Roget,A. and Téoule,R. (1992) Chemical synthesis of a biologically active natural tRNA with its minor bases. *Nucleic Acids Res.*, **20**, 5159–5166.
47. Audebert,M., Radicella,J.P. and Dizdaroglu,M. (2000) Effect of single mutations in the OGG1 gene found in human tumors on the substrate specificity of the Ogg1 protein. *Nucleic Acids Res.*, **28**, 2672–2678.
48. Fantini,D., Vascotto,C., Marasco,D., D'Ambrosio,C., Romanello,M., Vitagliano,L., Pedone,C., Poletto,M., Cesaratto,L., Quadrifoglio,F. *et al.* (2010) Critical lysine residues within the overlooked N-terminal domain of human APE1 regulate its biological functions. *Nucleic Acids Res.*, **38**, 8239–8256.
49. Erzberger,J.P. and Wilson,D.M. (1999) The role of Mg 2+ and specific amino acid residues in the catalytic reaction of the major human abasic endonuclease: new insights from EDTA-resistant incision of acyclic abasic site analogs and site-directed mutagenesis. *J. Mol. Biol.*, **290**, 447–457.
50. Chon,H., Vassilev,A., DePamphilis,M.L., Zhao,Y., Zhang,J., Burgers,P.M., Crouch,R.J. and Cerritelli,S.M. (2009) Contributions of the two accessory subunits, RNASEH2B and RNASEH2C, to the activity and properties of the human RNase H2 complex. *Nucleic Acids Res.*, **37**, 96–110.
51. Chon,H., Sparks,J.L., Rychlik,M., Nowotny,M., Burgers,P.M., Crouch,R.J. and Cerritelli,S.M. (2013) RNase H2 roles in genome integrity revealed by unlinking its activities. *Nucleic Acids Res.*, **41**, 3130–3143.
52. Wilson,D.M. (2005) Ape1 abasic endonuclease activity is regulated by magnesium and potassium concentrations and is robust on alternative DNA structures. *J. Mol. Biol.*, **345**, 1003–1014.
53. Poletto,M., Malfatti,M.C., Dorjsuren,D., Scognamiglio,P.L., Marasco,D., Vascotto,C., Jadhav,A., Maloney,D.J., Wilson,D.M., Simeonov,A. *et al.* (2016) Inhibitors of the apurinic/apyrimidinic endonuclease 1 (APE1)/nucleophosmin (NPM1) interaction that display anti-tumor properties. *Mol. Carcinog.*, **55**, 688–704.
54. Beernink,P.T., Segelke,B.W., Hadi,M.Z., Erzberger,J.P., Wilson,D.M. and Rupp,B. (2001) Two divalent metal ions in the active site of a new crystal form of human apurinic/apyrimidinic endonuclease, ape1: implications for the catalytic mechanism. *J. Mol. Biol.*, **307**, 1023–1034.
55. Izumi,T., Brown,D.B., Naidu,C.V., Bhakat,K.K., MacInnes,M.A., Saito,H., Chen,D.J. and Mitra,S. (2005) Two essential but distinct functions of the mammalian abasic endonuclease. *Proc. Natl. Acad. Sci. U.S.A.*, **102**, 5739–5743.
56. Rai,G., Vyjayanti,V.N., Dorjsuren,D., Simeonov,A., Jadhav,A., Wilson,D.M. and Maloney,D.J. (2013) Small molecule inhibitors of the human apurinic/apyrimidinic endonuclease 1 (APE1).
57. Boiteux,S. and Radicella,J.P. (2000) The human OGG1 gene: structure, functions, and its implication in the process of carcinogenesis. *Arch. Biochem. Biophys.*, **377**, 1–8.
58. Boiteux,S. and Radicella,J.P. (1999) Base excision repair of 8-hydroxyguanine protects DNA from endogenous oxidative stress. *Biochimie*, **81**, 59–67.
59. David,S.S., O'Shea,V.L. and Kundu,S. (2007) Base-excision repair of oxidative DNA damage. *Nature*, **447**, 941–950.
60. Chou,K.-m. and Cheng,Y.-c. (2003) The exonuclease activity of human apurinic/apyrimidinic endonuclease (APE1): biochemical properties and inhibition by the natural dinucleotide Gp4G. *J. Biol. Chem.*, **278**, 18289–18296.
61. Yasui,A. (2013) Alternative excision repair pathways. *Cold Spring Harb. Perspect. Biol.*, **5**, a012617.
62. Prorok,P., Alili,D., Saint-Pierre,C., Gasparutto,D., Zharkov,D.O., Ishchenko,A.A., Tudek,B. and Saparbaev,M.K. (2013) Uracil in

duplex DNA is a substrate for the nucleotide incision repair pathway in human cells. *Proc. Natl. Acad. Sci. U.S.A.*., **110**, E3695–E3703.
63. Hovatter,K.R. and Martinson,H.G. (1987) Ribonucleotide-induced helical alteration in DNA prevents nucleosome formation. *Proc. Natl. Acad. Sci. U.S.A.*, **84**, 1162–1166.
64. Potenski,C.J. and Klein,H.L. (2014) How the misincorporation of ribonucleotides into genomic DNA can be both harmful and helpful to cells. *Nucleic Acids Res.*, doi:10.1093/nar/gku773.
65. Sparks,J.L., Chon,H., Cerritelli,S.M., Kunkel,T.A., Johansson,E., Crouch,R.J. and Burgers,P.M. (2012) RNase H2-initiated ribonucleotide excision repair. *Mol. Cell*, **47**, 980–986.
66. Heider,M.R., Burkhart,B.W., Santangelo,T.J. and Gardner,A.F. (2017) Defining the RNaseH2 enzyme-initiated ribonucleotide excision repair pathway in archaea. *J. Biol. Chem.*, **292**, 8835–8845.
67. Hiller,B., Achleitner,M., Glage,S., Naumann,R., Behrendt,R. and Roers,A. (2012) Mammalian RNase H2 removes ribonucleotides from DNA to maintain genome integrity. *J. Exp. Med.*, **209**, 1419–1426.
68. Rice,G.I., Reijns,M.A.M., Coffin,S.R., Forte,G.M.A., Anderson,B.H., Szynkiewicz,M., Gornall,H., Gent,D., Leitch,A., Botella,M.P. *et al.* (2013) Synonymous mutations in *RNASEH2A* create cryptic splice sites impairing RNase H2 enzyme function in Aicardi-Goutières Syndrome. *Hum. Mutat.*, **34**, 1066–1070.
69. Pizzi,S., Sertic,S., Orcesi,S., Cereda,C., Bianchi,M., Jackson,A.P., Lazzaro,F., Plevani,P. and Muzi-Falconi,M. (2014) Reduction of hRNase H2 activity in Aicardi-Goutieres syndrome cells leads to replication stress and genome instability. *Hum. Mol. Genet.*, doi:10.1093/hmg/ddu485.
70. Moreira,P.I., Nunomura,A., Nakamura,M., Takeda,A., Shenk,J.C., Aliev,G., Smith,M.A. and Perry,G. (2008) Nucleic acid oxidation in Alzheimer disease. *Free Radic. Biol. Med.*, **44**, 1493–1505.
71. Loeb,L.A. and Preston,B.D. (1986) Mutagenesis by apurinic/apyrimidinic sites. *Annu. Rev. Genet.*, **20**, 201–230.
72. Jobert,L. and Nilsen,H. (2014) Regulatory mechanisms of RNA function: emerging roles of DNA repair enzymes. *Cell. Mol. Life Sci.*, doi:10.1007/s00018-014-1562-y.
73. Kochetkov,N.K. and Budovskii,E.I. (1972) Hydrolysis of N-glycosidic bonds in nucleosides, nucleotides, and their derivatives. In: Kochetkov,NK and Budovskii,EI (eds). *Organic Chemistry of Nucleic Acids*. Springer, Boston, pp. 425–448.
74. Lindahl,T. and Nyberg,B. (1972) Rate of depurination of native deoxyribonucleic acid. *Biochemistry (Mosc.)*, **11**, 3610–3618.
75. Kupfer,P.A. and Leumann,C.J. (2006) The chemical stability of abasic RNA compared to abasic DNA. *Nucleic Acids Res.*, **35**, 58–68.
76. Parsons,J.L., Dianova,I.I., Khoronenkova,S.V., Edelmann,M.J., Kessler,B.M. and Dianov,G.L. (2011) USP47 is a deubiquitylating enzyme that regulates base excision repair by controlling steady-state levels of DNA polymerase β. *Mol. Cell*, **41**, 609–615.
77. Sassa,A., Çağlayan,M., Rodriguez,Y., Beard,W.A., Wilson,S.H., Nohmi,T., Honma,M. and Yasui,M. (2016) Impact of ribonucleotide backbone on translesion synthesis and repair of 7,8-dihydro-8-oxoguanine. *J. Biol. Chem.*, doi:10.1074/jbc.M116.738732.
78. Vascotto,C., Cesaratto,L., Zeef,L.A.H., Deganuto,M., D'Ambrosio,C., Scaloni,A., Romanello,M., Damante,G., Taglialatela,G., Delneri,D. *et al.* (2009) Genome-wide analysis and proteomic studies reveal APE1/Ref-1 multifunctional role in mammalian cells. *Proteomics*, **9**, 1058–1074.
79. Simms,C.L. and Zaher,H.S. (2016) Quality control of chemically damaged RNA. *Cell. Mol. Life Sci.*, **73**, 3639–3653.
80. Rhee,Y., Valentine,M.R. and Termini,J. (1995) Oxidative base damage in RNA detected by reverse transcriptase. *Nucleic Acids Res.*, **23**, 3275–3282.
81. Shan,X., Chang,Y. and Lin,C.-l. G. (2007) Messenger RNA oxidation is an early event preceding cell death and causes reduced protein expression. *FASEB J.*, **21**, 2753–2764.
82. Tanaka,M., Chock,P.B. and Stadtman,E.R. (2007) Oxidized messenger RNA induces translation errors. *Proc. Natl. Acad. Sci. U.S.A.*, **104**, 66–71.
83. Hudak,K.A., Bauman,J.D. and Tumer,N.E. (2002) Pokeweed antiviral protein binds to the cap structure of eukaryotic mRNA and depurinates the mRNA downstream of the cap. *RNA*, **8**, 1148–1159.
84. Calabretta,A., Kupfer,P.A. and Leumann,C.J. (2015) The effect of RNA base lesions on mRNA translation. *Nucleic Acids Res.*, doi:10.1093/nar/gkv377.
85. Rychlik,M.P., Chon,H., Cerritelli,S.M., Klimek,P., Crouch,R.J. and Nowotny,M. (2010) Crystal structures of RNase H2 in complex with nucleic acid reveal the mechanism of RNA-DNA junction recognition and cleavage. *Mol. Cell*, **40**, 658–670.
86. Freudenthal,B.D., Beard,W.A., Cuneo,M.J., Dyrkheeva,N.S. and Wilson,S.H. (2015) Capturing snapshots of APE1 processing DNA damage. *Nat. Struct. Mol. Biol.*, **22**, 924–931.
87. Schramm,V.L. (1997) Enzymatic N-riboside scission in RNA and RNA precursors. *Curr. Opin. Chem. Biol.*, **1**, 323–331.
88. Hayakawa,H., Uchiumi,T., Fukuda,T., Ashizuka,M., Kohno,K., Kuwano,M. and Sekiguchi,M. (2002) Binding capacity of human YB-1 protein for RNA containing 8-oxoguanine. *Biochemistry (Mosc.)*, **41**, 12739–12744.
89. Vidal,A.E., Hickson,I.D., Boiteux,S. and Radicella,J.P. (2001) Mechanism of stimulation of the DNA glycosylase activity of hOGG1 by the major human AP endonuclease: bypass of the AP lyase activity step. *Nucleic Acids Res.*, **29**, 1285–1292.
90. Woo,J., Park,H., Sung,S.H., Moon,B.-I., Suh,H. and Lim,W. (2014) Prognostic value of human apurinic/apyrimidinic endonuclease 1 (APE1) expression in breast cancer. *PLoS ONE*, **9**, e99528.
91. Al-Attar,A., Gossage,L., Fareed,K.R., Shehata,M., Mohammed,M., Zaitoun,A.M., Soomro,I., Lobo,D.N., Abbotts,R., Chan,S. *et al.* (2010) Human apurinic/apyrimidinic endonuclease (APE1) is a prognostic factor in ovarian, gastro-oesophageal and pancreatico-biliary cancers. *Br. J. Cancer*, **102**, 704–709.
92. Mol,C.D., Izumi,T., Mitra,S. and Tainer,J.A. (2000) DNA-bound structures and mutants reveal abasic DNA binding by APE1 and DNA repair coordination. *Nature*, **403**, 451–456.